



Memorial Sloan Kettering
Cancer Center

Cancer Imaging – Advanced Contrast Mechanisms in MRI

Kayvan R. Keshari, PhD
www.ski.edu/keshari
[@KeshariLab](https://twitter.com/KeshariLab)



The Plan

1. Revisiting Relaxation contrast (T_1 , T_2 and T_2^*)
 - a. BOLD and ASL
2. Diffusion-weighted MRI
3. Contrast Mechanisms for MRI
 - a. Relaxation based (small and large molecules)
 - b. Chemical Exchange Saturation Transfer
 - c. Magnetic Resonance Spectroscopy/Spectroscopic Imaging
 - d. Multi-nuclear MRS/MRI
 - Isotope tracing
 - Hyperpolarization



Memorial Sloan Kettering
Cancer Center

Discussion Papers and Background

Background paper:

- James, M. L. & Gambhir, S. S. A molecular imaging primer: modalities, imaging agents, and applications. *Physiological reviews* **92**, 897-965 (2012).

2 Discussion Papers:

- Day, S. E. *et al.* Detecting tumor response to treatment using hyperpolarized ¹³C magnetic resonance imaging and spectroscopy. *Nat Med* **13**, 1382–1387 (2007).
- Choi, C. *et al.* 2-hydroxyglutarate detection by magnetic resonance spectroscopy in IDH-mutated patients with gliomas. *Nat Med* **18**, 624–629 (2012).



Memorial Sloan Kettering
Cancer Center

Magnetic Resonance

- *Nuclear magnetic dipole* – charged particle spinning around an axis => small circular current...faster the nucleus spins => bigger the current

$$\vec{\mu} = \gamma \vec{I}$$

- Magnetic moment μ , spin angular momentum I , gyromagnetic ratio γ

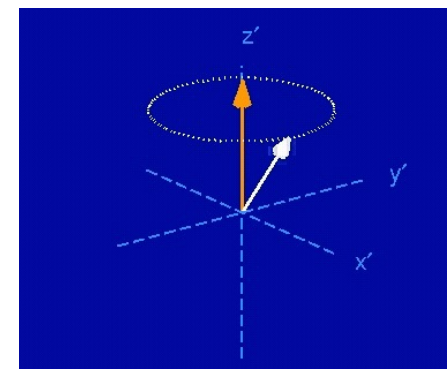
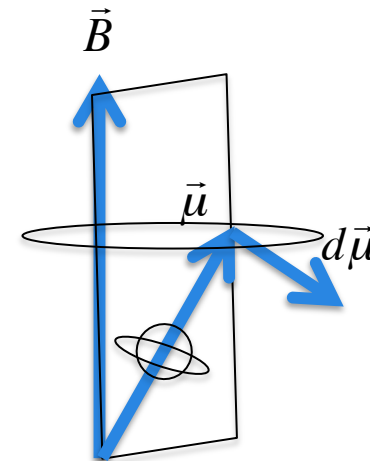
- When you put the nucleus in a field B , since the nucleus is spinning you have Larmor precession...

- Spins precess perpendicular to the plane

$$\frac{d\vec{\mu}}{dt} = -\gamma \vec{B} \wedge \vec{\mu}$$

- Typically we have a static field B_0 and define angular velocity of the precession and frequency (*Larmor freq*)...

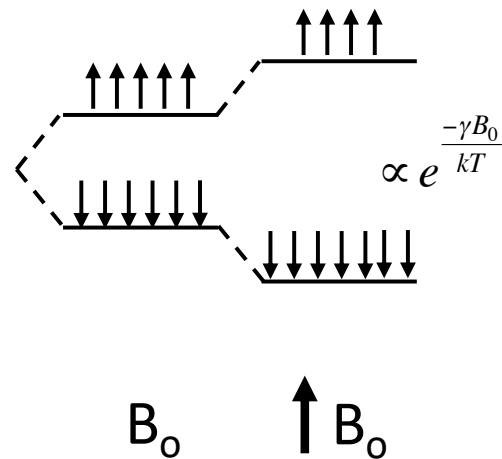
$$\omega_0 = \gamma B_0 \quad \nu_0 = \frac{\omega_0}{2\pi}$$



Memorial Sloan Kettering
Cancer Center

Magnetic Resonance

Signal depends on the Boltzmann Distribution (k), gamma, field, and temperature



Memorial Sloan Kettering
Cancer Center

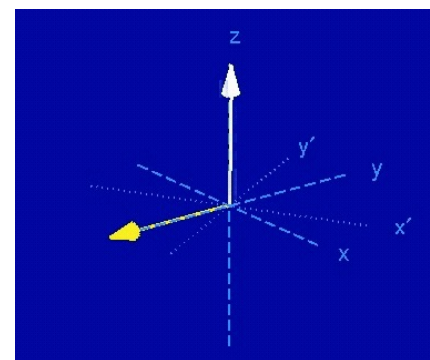
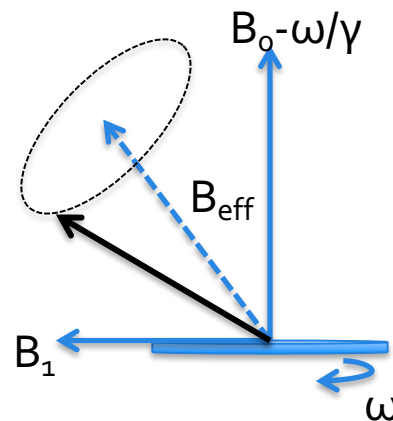
Revisiting Relaxation contrast (T_1 , T_2 and T_2^*)



Memorial Sloan Kettering
Cancer Center

Magnetic Resonance

- Problem...if the magnetization is on Z (main field) we can't observe it...
- RF Excitation
 - Tip M away from Z with B_1
 - Then M precesses around the new field (B_0+B_1)
 - Since we would need a lot of power to generate a static B_1 that would actually influence the overall B field...
 - We let the B_1 field rotate around B_0 with the same frequency as M...=> we excite at the frequency of M
- Flip angle $\alpha = \gamma B_1 t_p$



Memorial Sloan Kettering
Cancer Center

Magnetic Resonance

- Immediately after excitation, precession can't go on forever...
- Relaxation
 - T_1 – *spin-lattice*, restores Boltzmann $\Rightarrow M_z$ regrows
 - T_2 – *spin-spin*, a result of an ensemble of different magnetic dipoles $\Rightarrow M_{xy}$ decays
- Define the cross product in xyz.. And substitute our excitation scheme, B_0 and these relaxation coefficients...

Bloch Equations

$$\frac{d}{dt}M_x = -\gamma(B_yM_z - B_zM_y)$$

$$\frac{d}{dt}M_y = -\gamma(B_zM_x - B_xM_z)$$

$$\frac{d}{dt}M_z = -\gamma(B_xM_y - B_yM_x)$$

$$\vec{B} = \left[B_1, 0, B_0 - \frac{\omega}{\gamma} \right]$$

$$\frac{d}{dt}M_x = (\omega_0 - \omega)M_y - \frac{1}{T_2}M_x$$

$$\frac{d}{dt}M_y = -(\omega_0 - \omega)M_x - \frac{1}{T_2}M_y + \omega_1 M_z$$

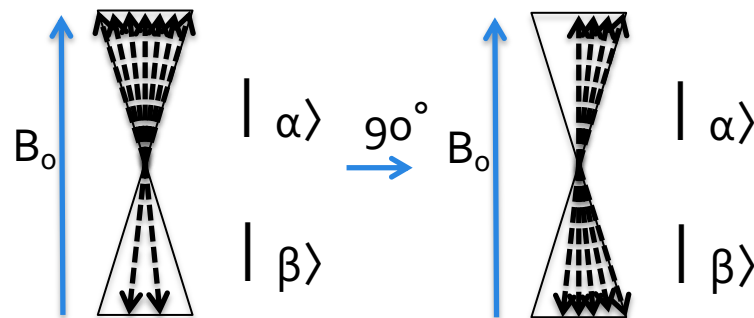
$$\frac{d}{dt}M_z = -\omega_1 M_y - \frac{1}{T_1}(M_z - M_0)$$



Memorial Sloan Kettering
Cancer Center

Magnetic Resonance – T_1

- T_1 relaxation – spin-lattice
 - Spins exchange energy via “on resonance” fluctuations with the lattice
 - More fundamental... $|\alpha\rangle$ and $|\beta\rangle$ need to go through transitions to re-establish equilibrium



- For this to happen, spins have exchange energy with the surroundings... *lattice*
- This is dependent on the local field the spin experiences

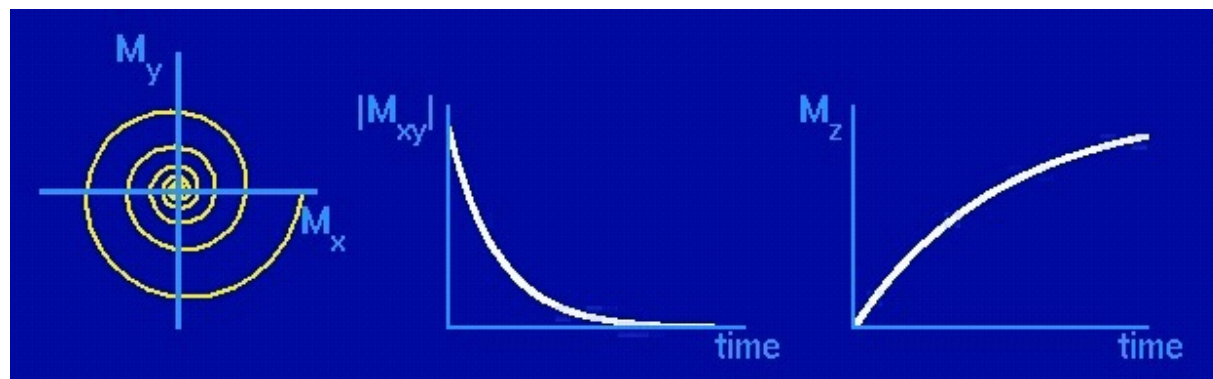
$$\frac{d}{dt} M_z = -\frac{1}{T_1} (M_z - M_0) \quad \xrightarrow{\text{ode}} \quad M_z(t) = M_0 [1 - e^{-\frac{t}{T_1}}]$$



Memorial Sloan Kettering
Cancer Center

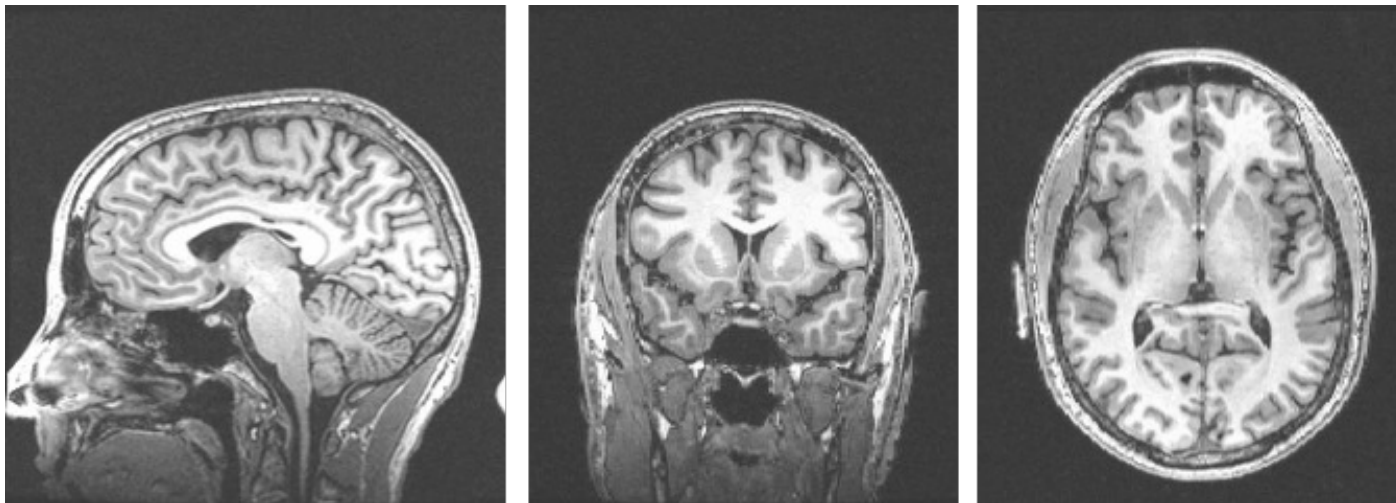
Magnetic Resonance - Relaxation

- Immediately after excitation, precession can't go on forever...
- Relaxation
 - T_1 – *spin-lattice*, restores Boltzmann $\Rightarrow M_z$ regrows
 - Spins exchange energy via “on resonance” fluctuations with the lattice
 - T_2 – *spin-spin*, a result of an ensemble of different magnetic dipoles $\Rightarrow M_{xy}$ decays
 - Spins “feel” magnetic fields from other molecules and become off frequency with respect to B_0 and other spins



Memorial Sloan Kettering
Cancer Center

T₁-weighted imaging



Dark on T₁-weighted image:

- increased water, as in edema, tumor, infarction, inflammation, infection, hemorrhage
- low proton density, calcification
- flow void

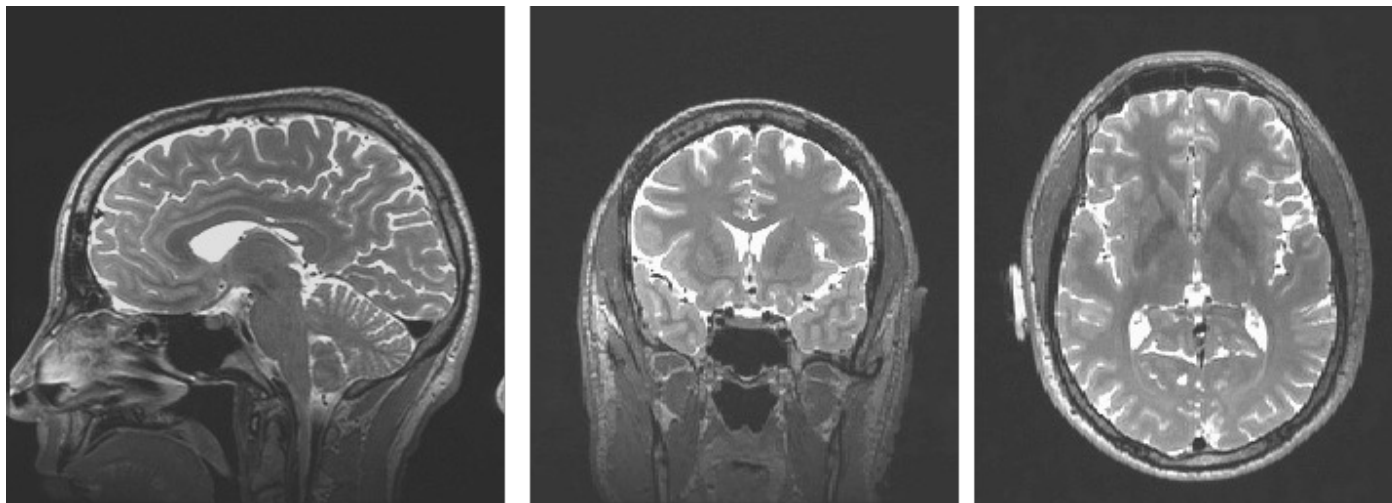
Bright on T₁-weighted image:

- fat
- subacute hemorrhage, protein-rich fluids
- paramagnetic substances: gadolinium, manganese, copper



Memorial Sloan Kettering
Cancer Center

T₂-weighted imaging



Bright on T₂-weighted image:

- increased water, as in edema, tumor, infarction, inflammation, infection, subdural collection
- methemoglobin (extracellular) in subacute hemorrhage

Dark on T₂-weighted image:

- low proton density, calcification, fibrous tissue
- paramagnetic substances: deoxyhemoglobin, methemoglobin (intracellular), iron
- protein-rich fluid
- flow void



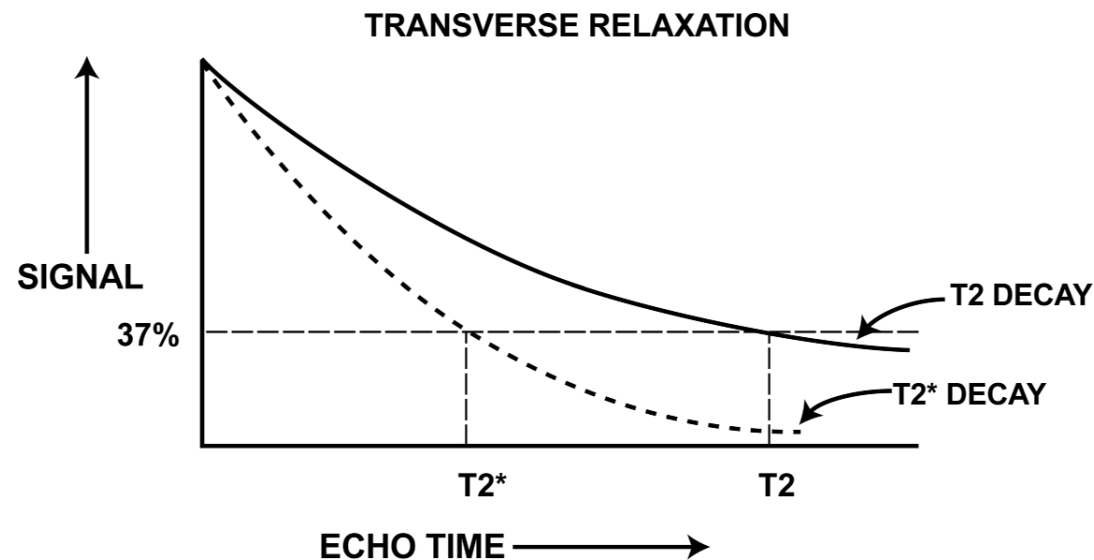
Memorial Sloan Kettering
Cancer Center

So then what is T_2^*

The local magnetic field is actually not homogenous causing additional relaxation

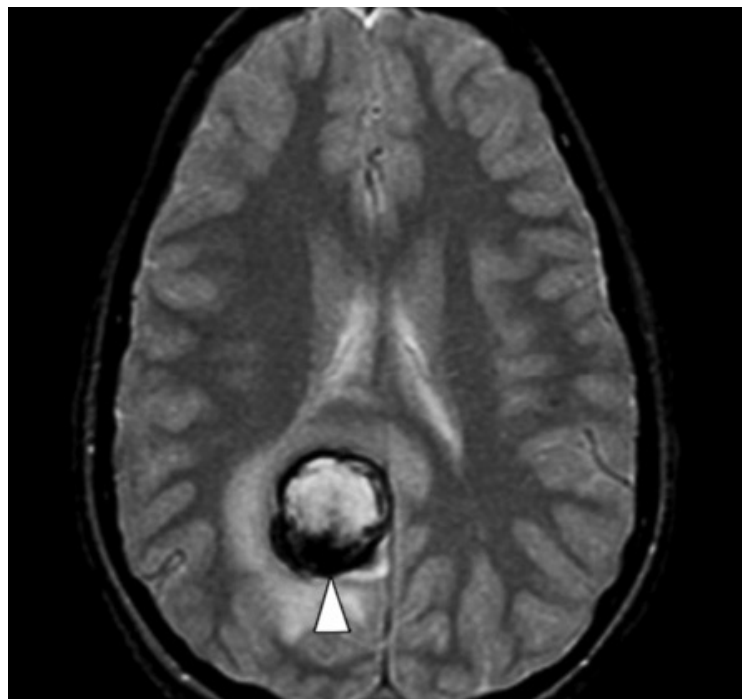
$$\frac{1}{T_2^*} = \frac{1}{T_2} + \frac{1}{T_2'}$$

$$\frac{1}{T_2'} = \gamma \Delta B_{inhom}$$



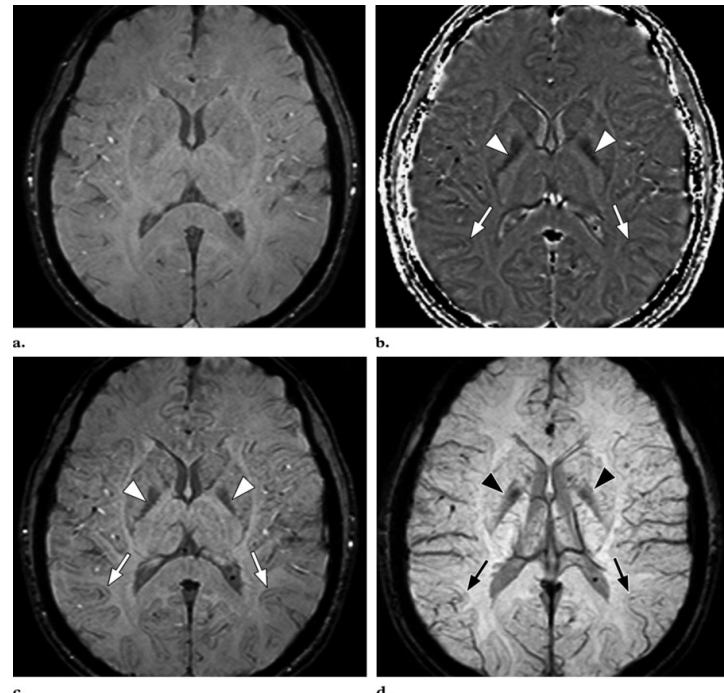
Memorial Sloan Kettering
Cancer Center

T_2^* -weighted imaging



Blood causes local T_2^*

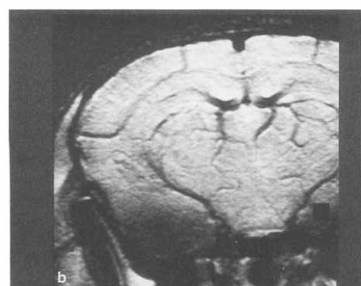
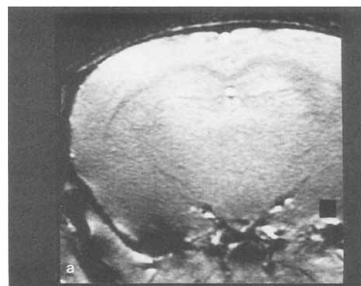
Susceptibility weighted imaging (SWI)



Memorial Sloan Kettering
Cancer Center

BOLD?

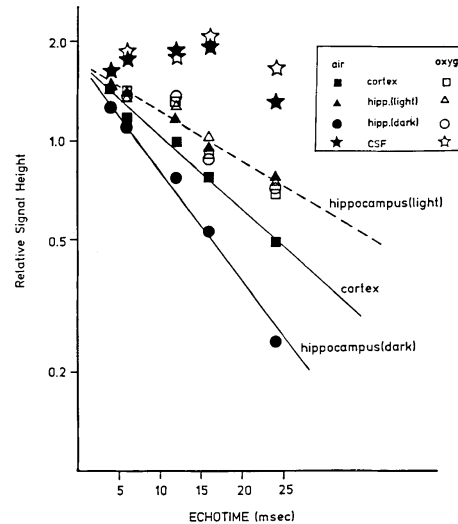
Breathing 100% oxygen



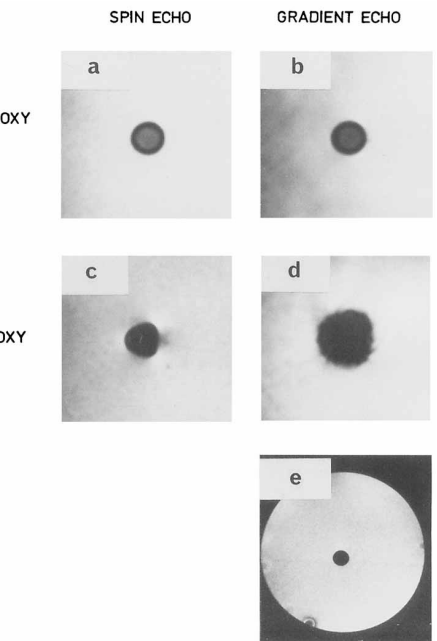
Breathing normal air



Ogawa et al. MRM 1990



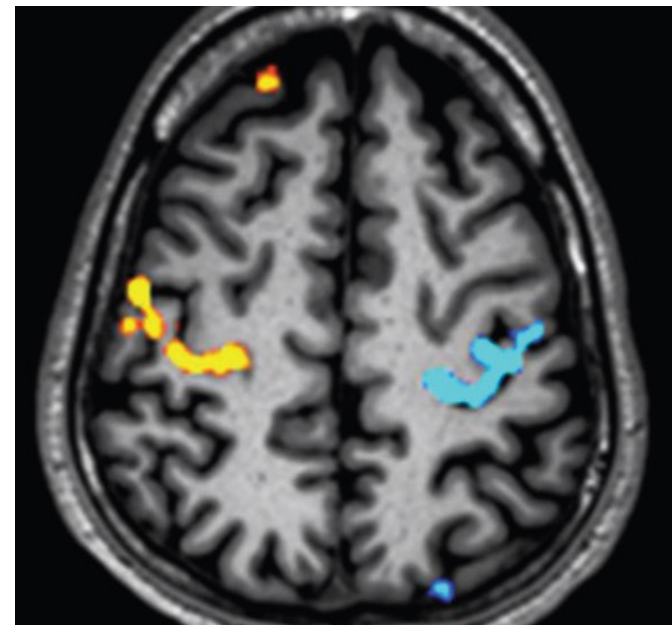
Signal decay as a function of echo time in gradient echo images



Memorial Sloan Kettering
Cancer Center

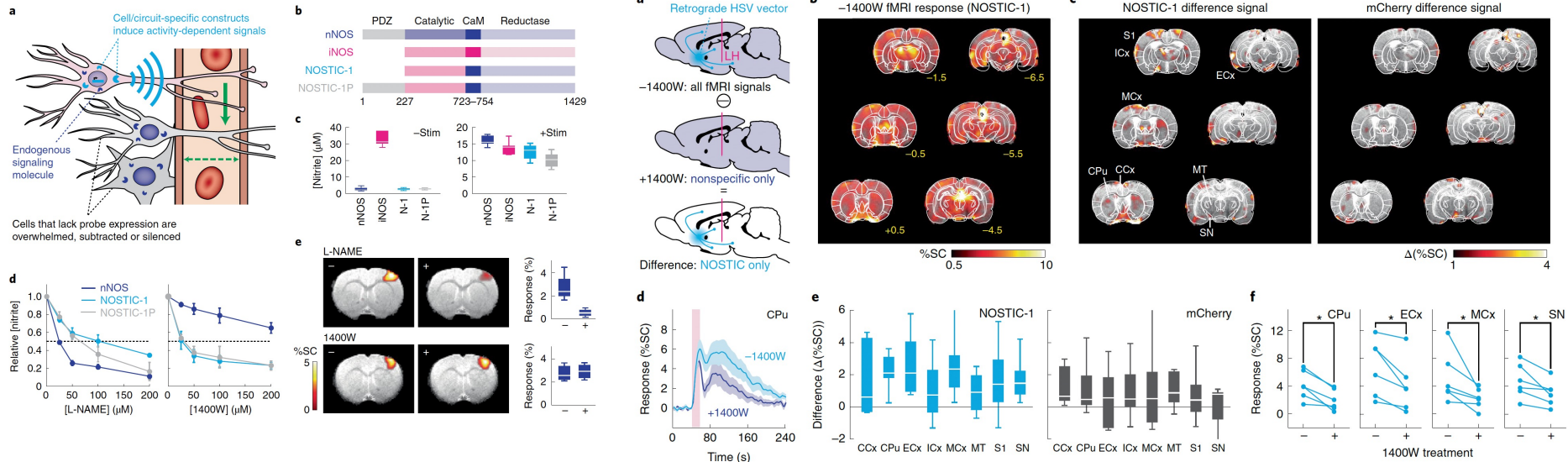
BOLD → fMRI

- Oxyhemoglobin is diamagnetic while deoxyhemoglobin is paramagnetic relative to surrounding tissue
- Deoxyhemoglobin causes a reduction in signal by creating microscopic field gradients within and around the blood vessels
- Stimulation of a brain area cause increased cerebral blood flow to an area, increase in blood oxygen, decrease in deoxyhemoglobin and thus increase in local MR signal...we call this BOLD



Memorial Sloan Kettering
Cancer Center

Can you use **BOLD** to read out other mechanisms?



Ghosh et al. *Nature Neuro* 2022



Memorial Sloan Kettering
Cancer Center

Arterial Spin Labeling (ASL)

- What happens if you invert a moving spin and then observe in a given FOV?
- Think of it as a “spin-tag”

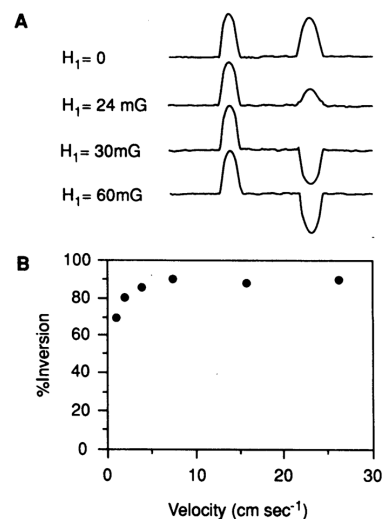


FIG. 1. Phantom studies on the effect of H_1 and velocity on spin inversion by adiabatic fast passage. (A) One-dimensional intensity profiles of a phantom consisting of stationary blood (left) and flowing blood (right), respectively, as a function of radiofrequency field strength, H_1 , used for inversion. The blood is flowing through a gradient of $0.5 \text{ G} \cdot \text{cm}^{-1}$. (B) Variation of degree of inversion in a phantom of flowing blood as a function of flow velocity. A gradient of $1.0 \text{ G} \cdot \text{cm}^{-1}$ and H_1 of 59 mG were used for all flow velocities.

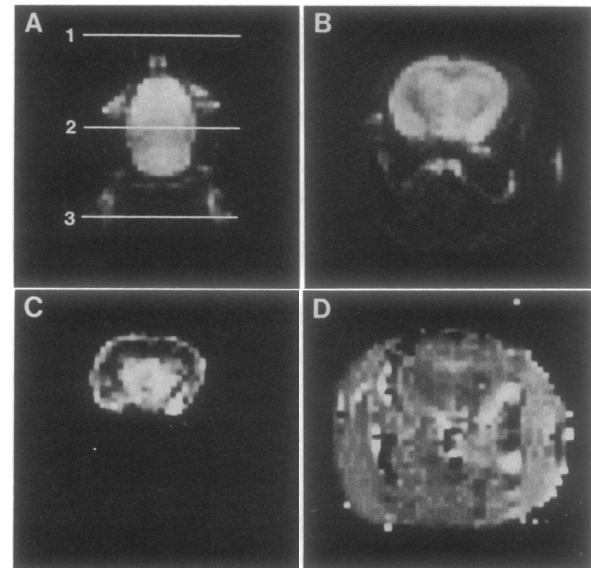


FIG. 2. (A) Coronal image of a rat head. The resonance planes for radiofrequency used for spin inversion by AFP for control and inversion images are indicated by 1 and 3, respectively, and plane 2 is the detection plane. (B) Control transverse image from the detection plane (plane 2 in A). (C) Difference image between control and inversion images. (D) $T_{1\text{app}}$ image.



Arterial Spin Labeling (ASL)

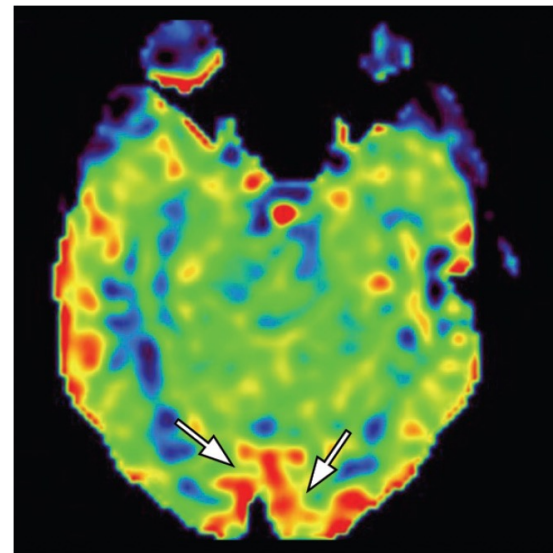
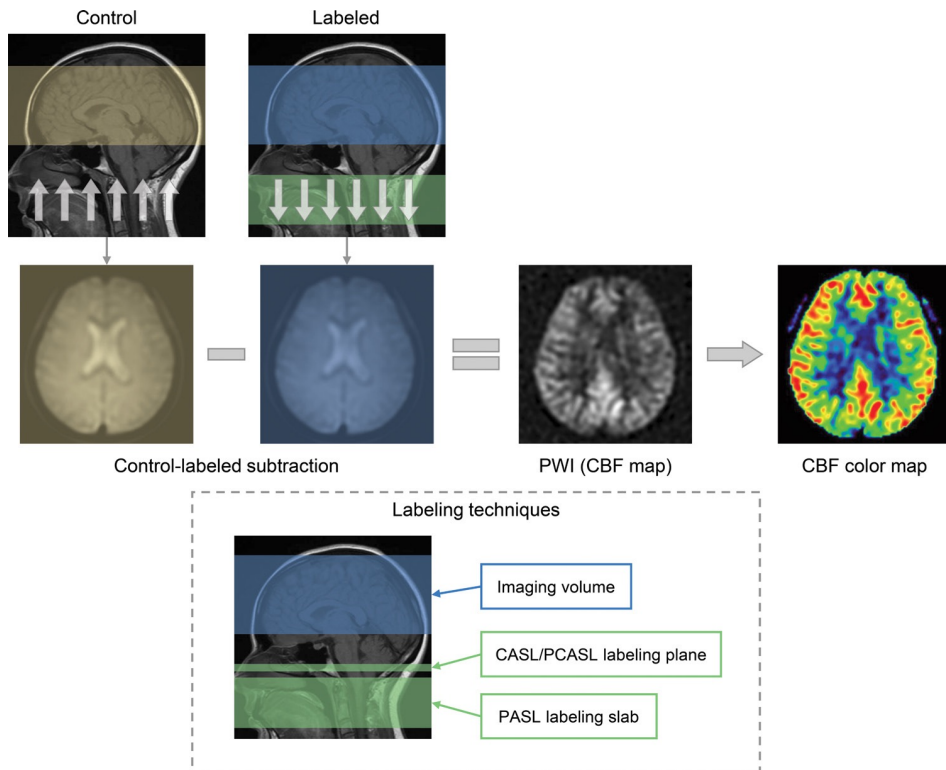


Figure 2. Occipital lobe hyperperfusion artifact in a healthy 32-year-old woman. ASL map shows bilateral and symmetric high signal intensity in the occipital lobes (arrows), which represents occipital lobe hyperperfusion artifacts that occurred because the patient opened her eyes during imaging.



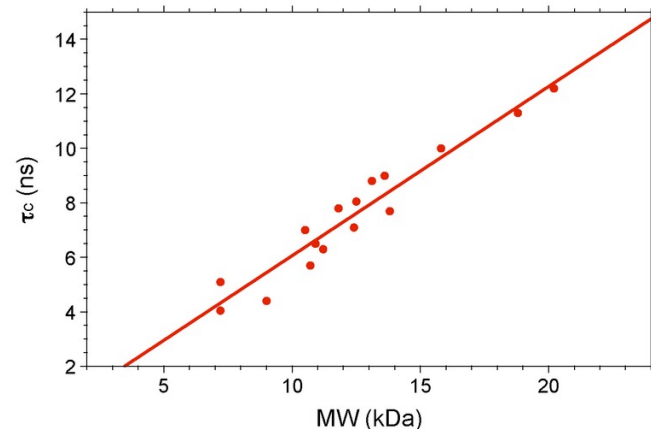
Magnetic Resonance – Molecules tumbling

Rotational correlation time

- Characteristic tumbling rate of a molecule, Brownian rotation diffusion of a particle
- Defined as time it takes a particle to rotate 1 radian
- Stoke's approx...

$$\tau_c = \frac{4\pi\eta r^3}{3kT} \quad r \approx \sqrt[3]{\frac{3M}{4\pi\rho N_a}} + r_w$$

η is the viscosity, r eff hydrodynamic radius
M, mass in kDa, ρ density,
 N_a avagadro, r_w = hydration (1-3A)

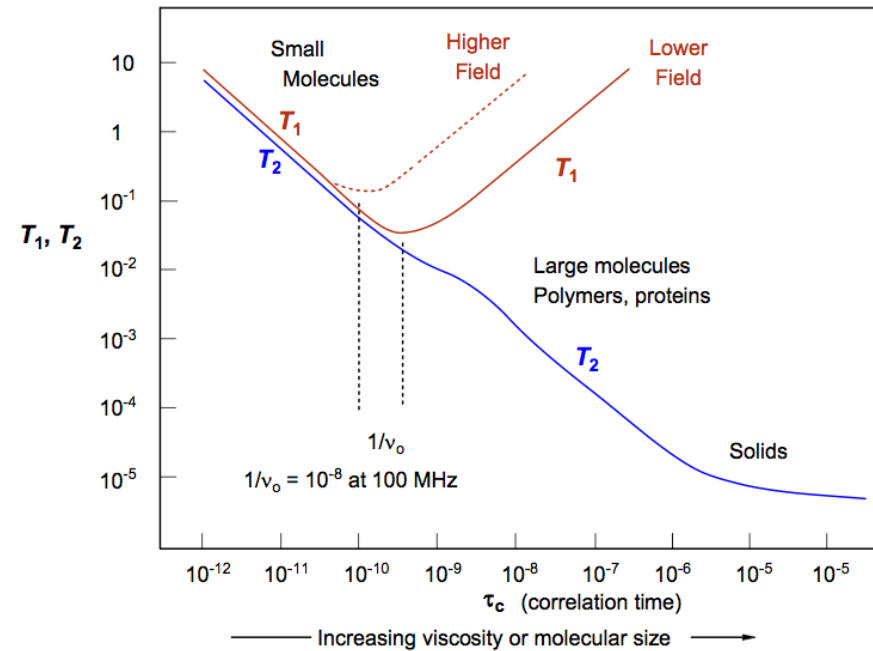


Memorial Sloan Kettering
Cancer Center

Magnetic Resonance – Correlation time

What does this have to do with NMR/MRI?

$$\frac{T_1}{T_2} = 1 + \frac{1}{2} \omega_0^2 \tau_c^2$$



Memorial Sloan Kettering
Cancer Center

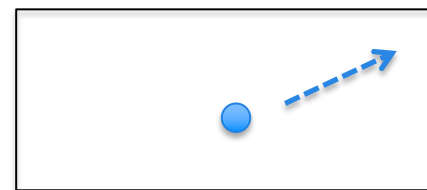
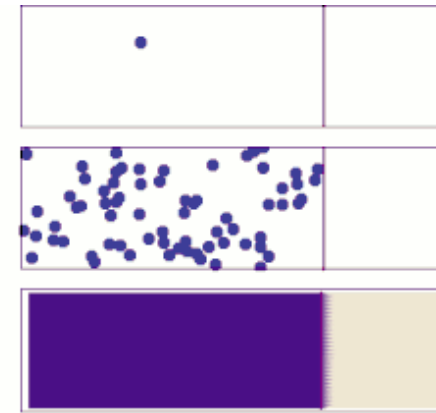
Diffusion-weighted MRI



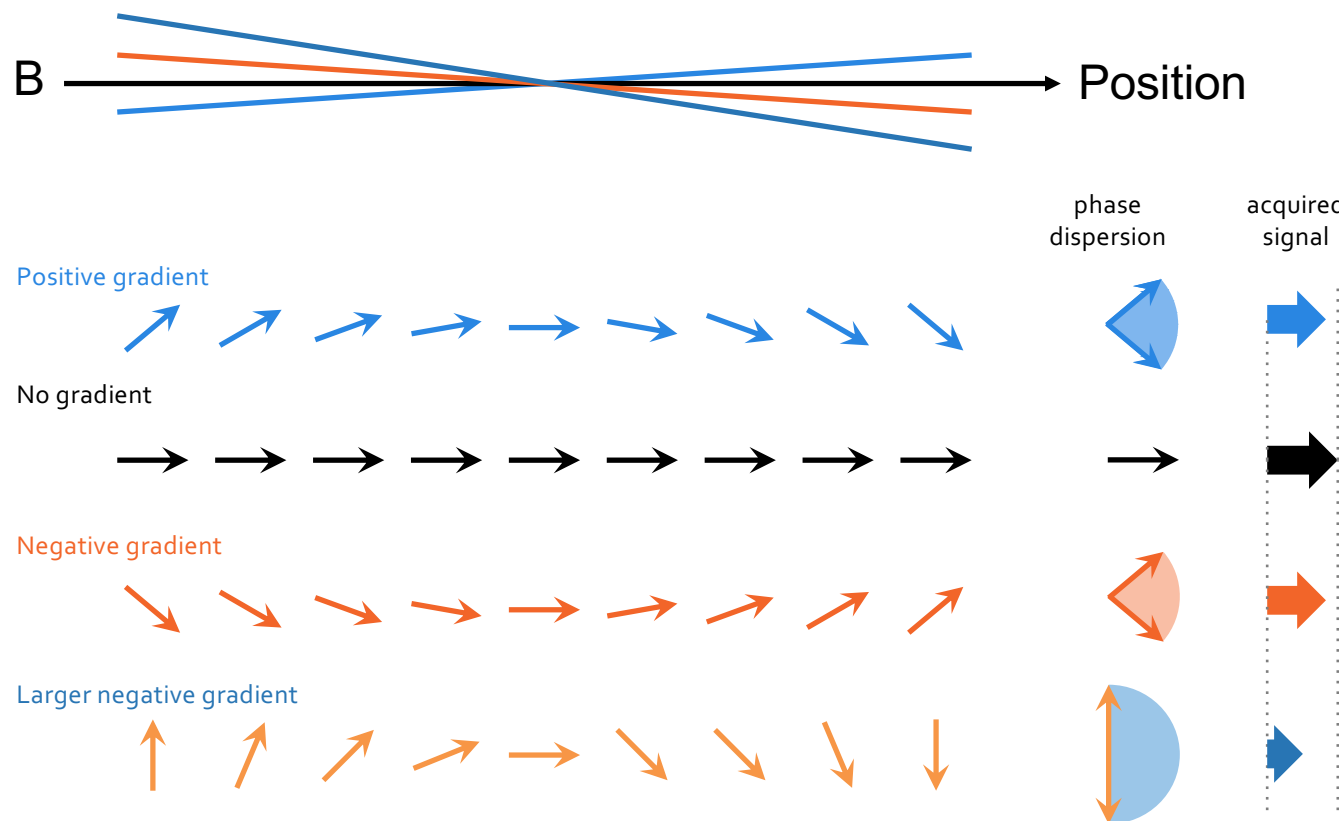
Memorial Sloan Kettering
Cancer Center

Magnetic Resonance – Diffusion

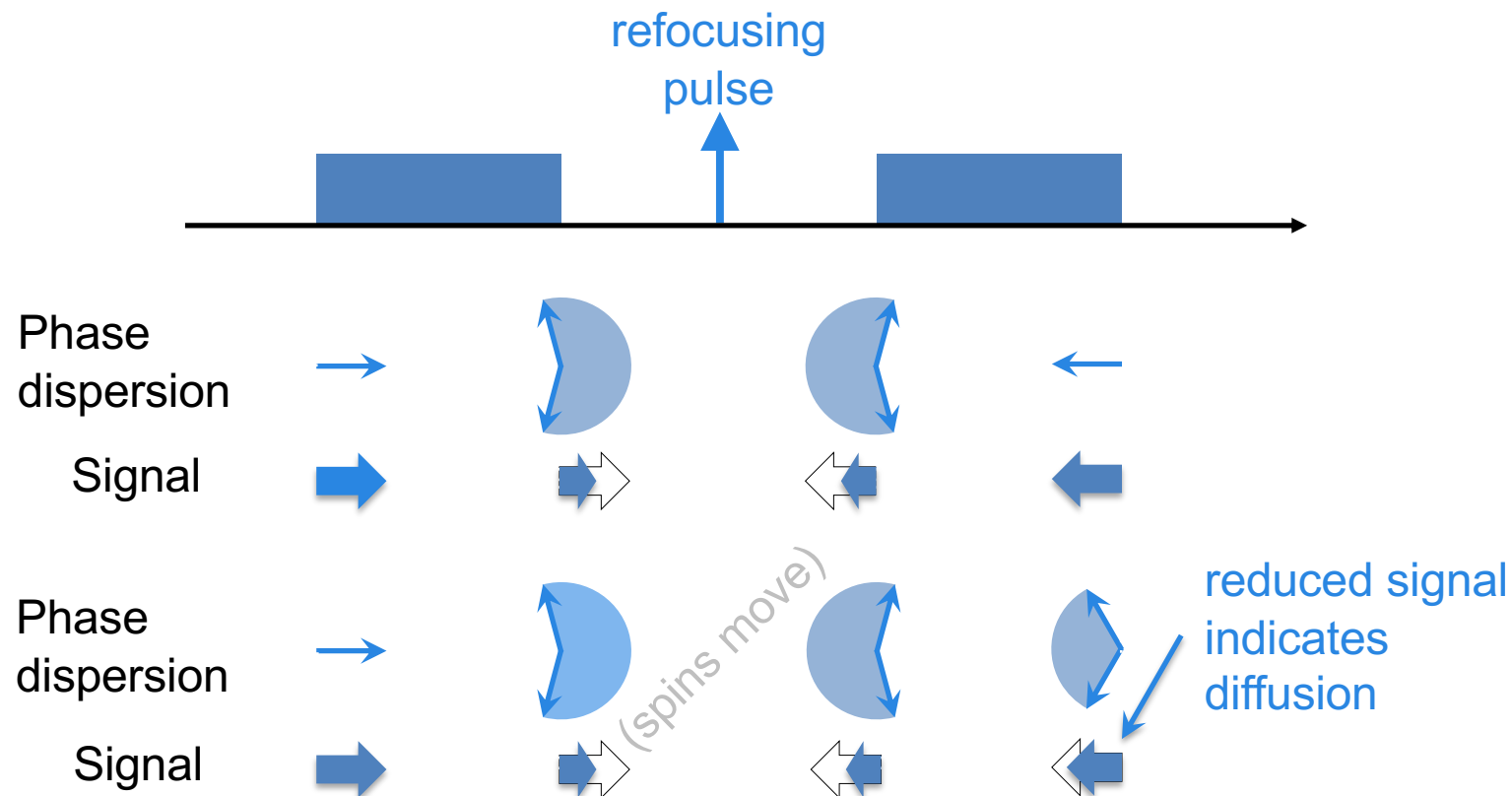
- Brownian motion – random movement of particles in a liquid
- What if they run into a wall?
- What if they travel a long distance?
- Can we encode that?



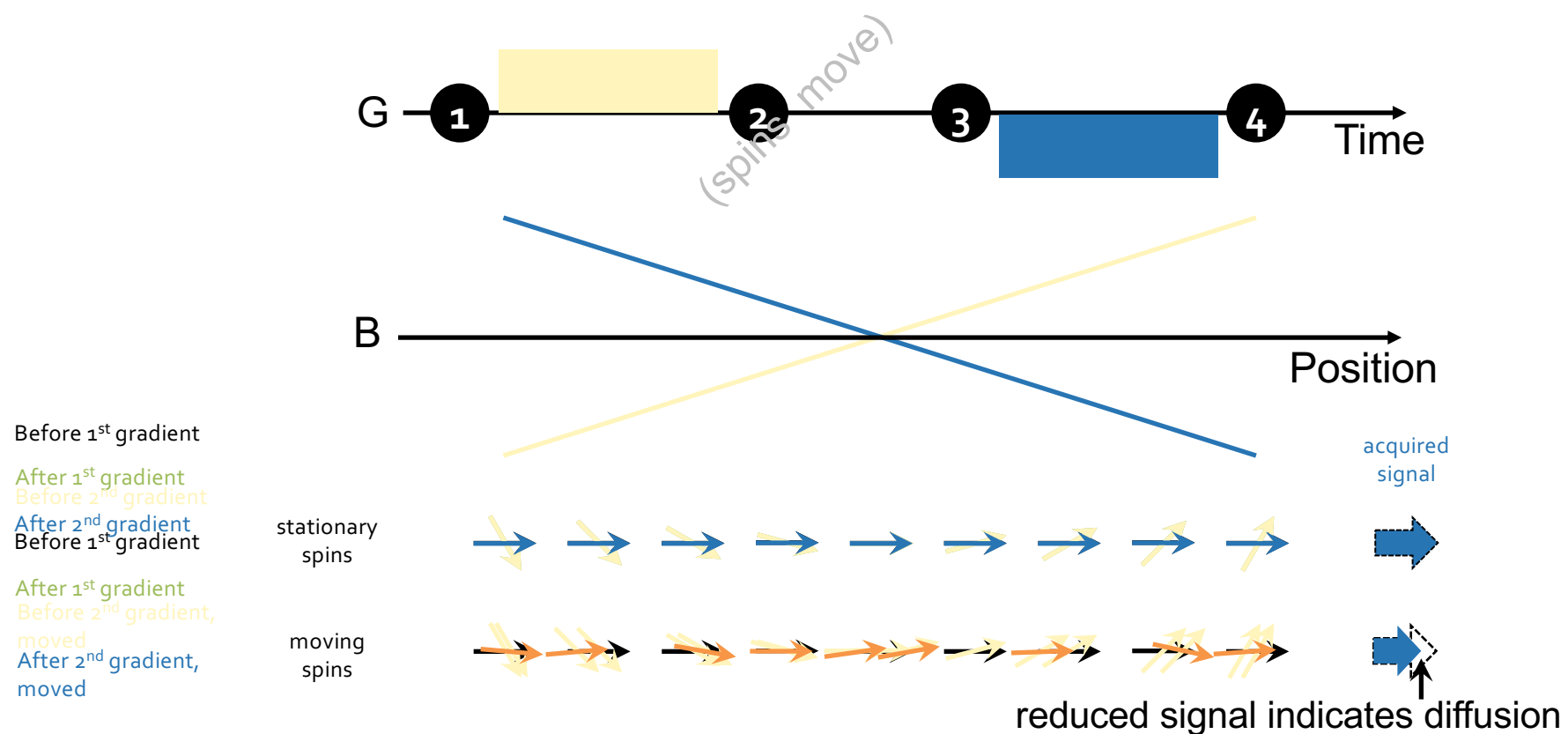
Gradients dephase spins within a voxel



Gradient pairs can be used to identify moving spins (spin echo sequence)



Gradient pairs can be used to identify moving spins (gradient echo sequence)



Basic DWI sequence

- Spin-echo EPI
 - Higher signal => restricted diffusion
 - b value describes the amount of diffusion-weighting for a given spin-echo sequence
 - Diffusion time (Δ) affects the range of diffusion differences

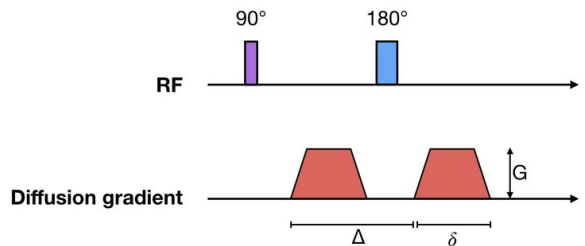


Memorial Sloan Kettering
Cancer Center

Quantification

b value

$$b = \gamma^2 G^2 \delta^2 (\Delta - \frac{\delta}{3})$$



γ = gyromagnetic ratio

G = magnitude of the two balanced DW gradient pulses

δ = width of the two balanced DW gradient pulses

Δ = time between the two balanced DW gradient pulses

Relationship between signal of $b = 0$, DWI and ADC

$$S_{DWI} = S_{b=0} \times e^{(-b \times D)}$$

equivalent to...

$$D = -\frac{1}{b} \times \ln\left(\frac{S_{DWI}}{S_{b=0}}\right)$$

S_{DWI} = signal intensity of isotropic DWI

$S_{b=0}$ = signal intensity of $b = 0$

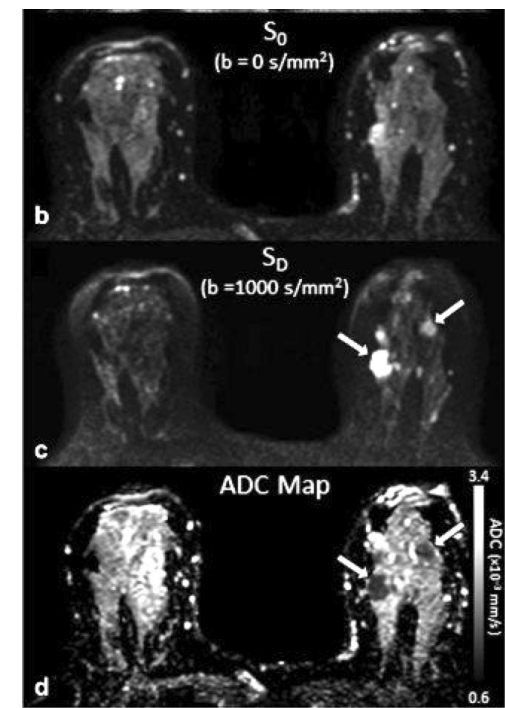
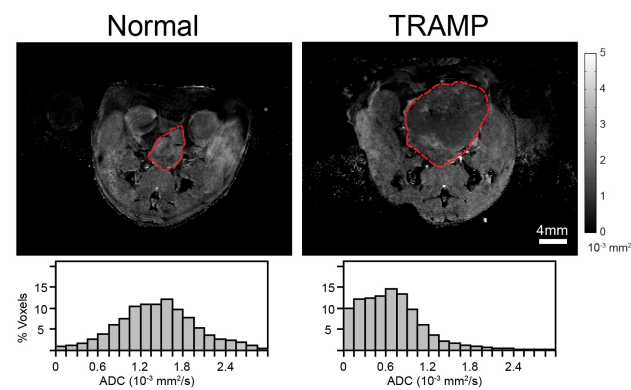
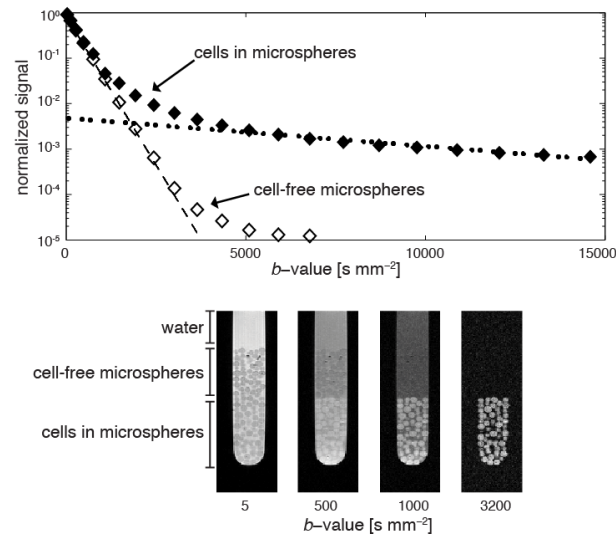
b = b value

D = apparent diffusion coefficient (ADC)



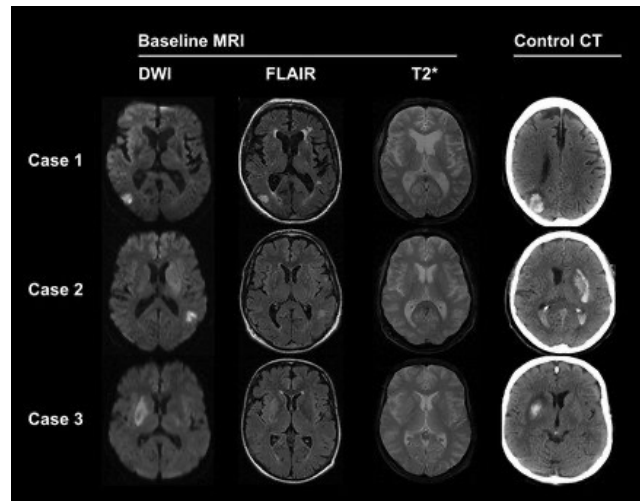
Memorial Sloan Kettering
Cancer Center

Magnetic Resonance – Diffusion *in vitro* and *in vivo*



Memorial Sloan Kettering
Cancer Center

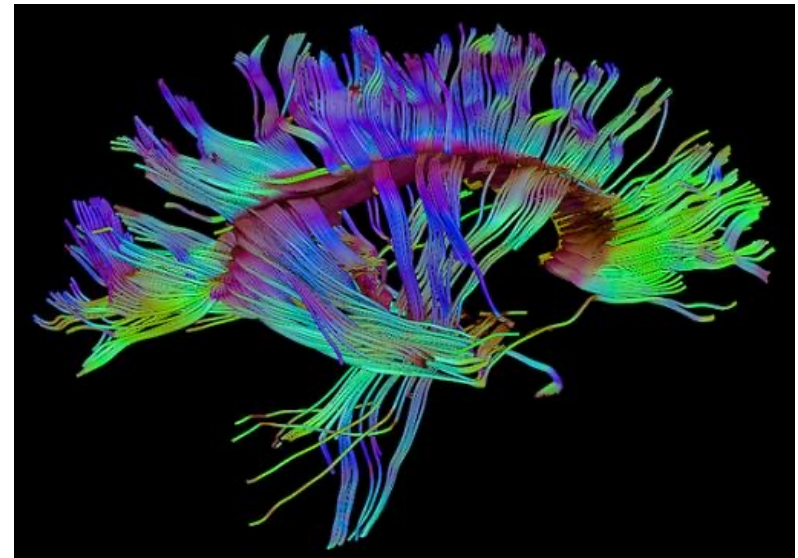
- Common applications
 - Ischemia
 - Edema
 - Cancer
- In vivo diffusion reflects
 - Cellularity
 - Structure (e.g., vessels, intracellular structures)
 - Presence of macromolecules and organelles



Memorial Sloan Kettering
Cancer Center

Advanced Applications

- Diffusion Tensor Imaging (DTI)
 - Multiple directions we calculate a tensor map...
 - measure diffusion anisotropy
- Intravoxel Incoherent Motion (IVIM) Imaging
 - separate perfusion and diffusion contributions
- Restriction Spectrum Imaging (RSI)
 - distinguish intra-cellular and extra-cellular components



Memorial Sloan Kettering
Cancer Center

Contrast Mechanisms for MRI

- a. Relaxation based (small and large molecules)
- b. Chemical Exchange Saturation Transfer
- c. Magnetic Resonance Spectroscopy/Spectroscopic Imaging
- d. Multi-nuclear MRS/MRI
 - Isotope tracing
 - Hyperpolarization



Memorial Sloan Kettering
Cancer Center

Contrast Mechanisms for MRI

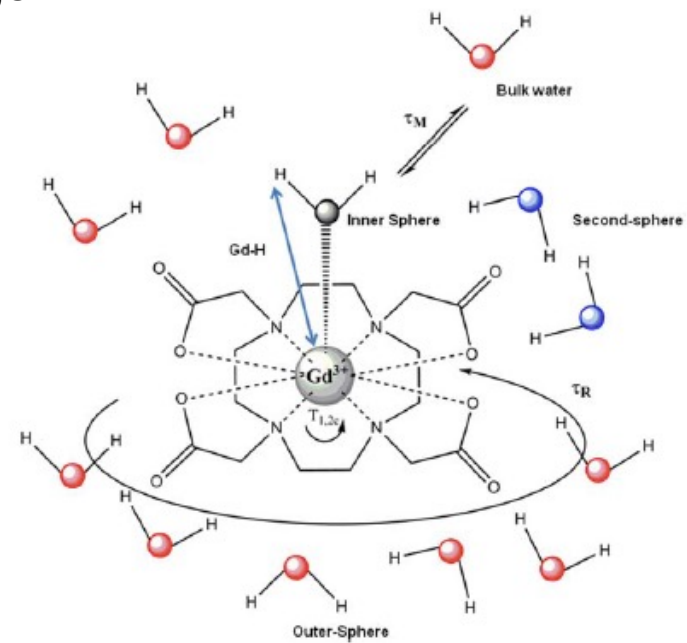
- a. Relaxation based (small and large molecules)
- b. Chemical Exchange Saturation Transfer
- c. Magnetic Resonance Spectroscopy/Spectroscopic Imaging
- d. Multi-nuclear MRS/MRI
 - Isotope tracing
 - Hyperpolarization



Memorial Sloan Kettering
Cancer Center

T_1 -Based Contrast Agents

- Shortening longitudinal relaxation time of water
- “positive agent”, brightening T_1 -weighted image sequences
- Gd^{3+} in lanthanide(Ln) family of elements
 - Seven unpaired electrons in 4f orbital
 - Very high magnetic moment
 - Unusual long electronic spin relaxation time



J Magn Reson Imaging. 2015 Sep;42(3):545-65

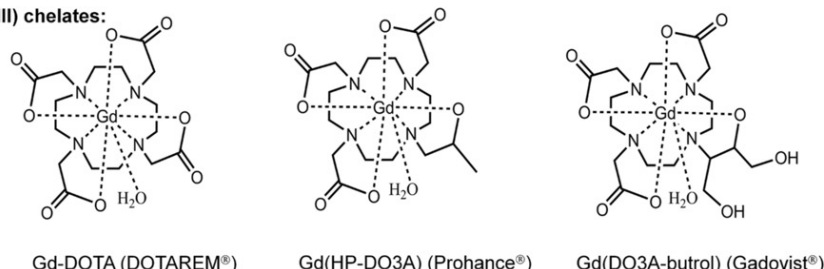


Memorial Sloan Kettering
Cancer Center

Perfusion – Gd^{3+} MRI

- Gd^{3+} chelates – change shorten T_1 relaxation

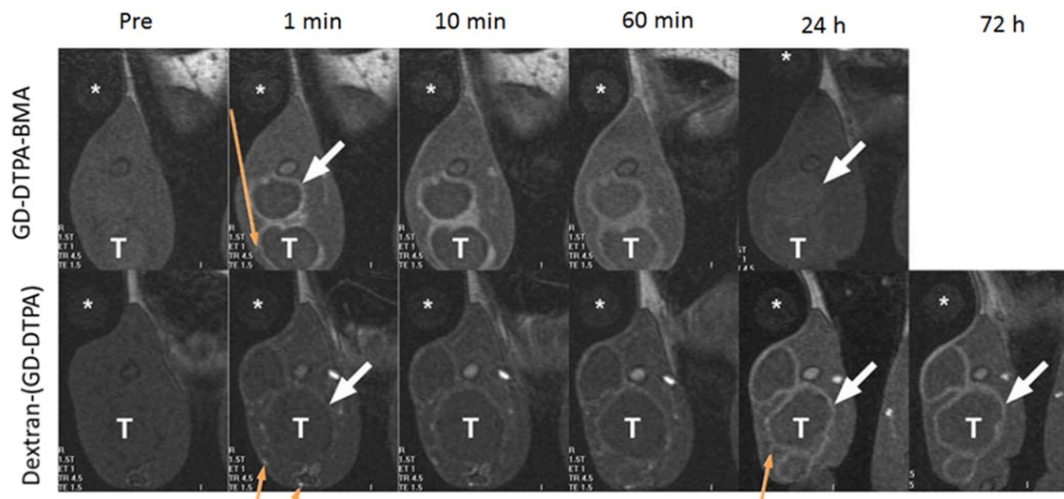
Macrocyclic $\text{Gd}(\text{III})$ chelates:



Gd-DOTA (DOTAREM®)

Gd(HP-DO3A) (Prohance®)

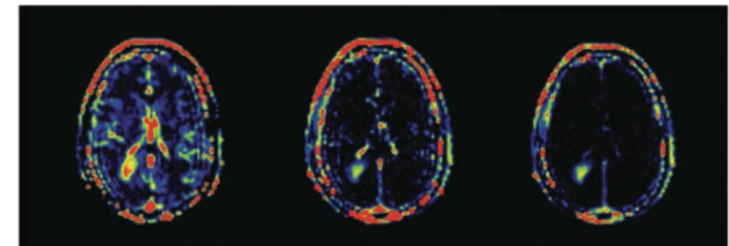
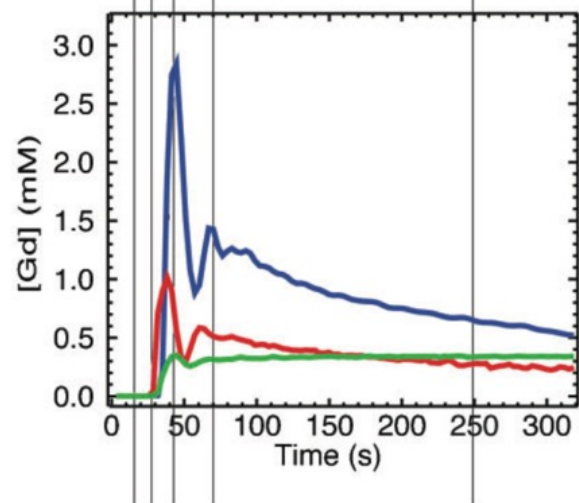
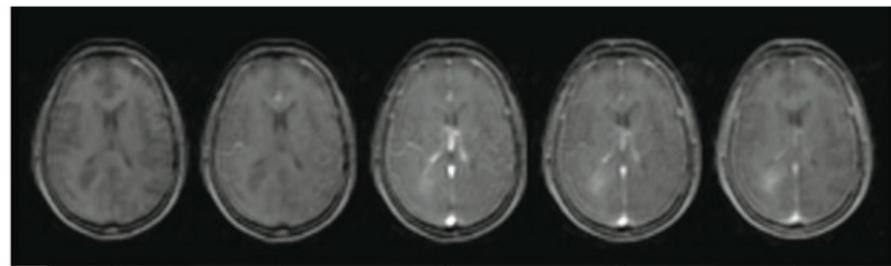
Gd(DO3A-butrol) (Gadovist®)



Memorial Sloan Kettering
Cancer Center

1884

Perfusion – Gd^{3+} MRI



V_p
Blood pool volume

V_e
extracellular
distribution
space

K_{trans}
Perfusion “rate”

O'connor et al 2011



Memorial Sloan Kettering
Cancer Center

Can we exploit T_2^* - Super Paramagnetic Iron (SPIO)

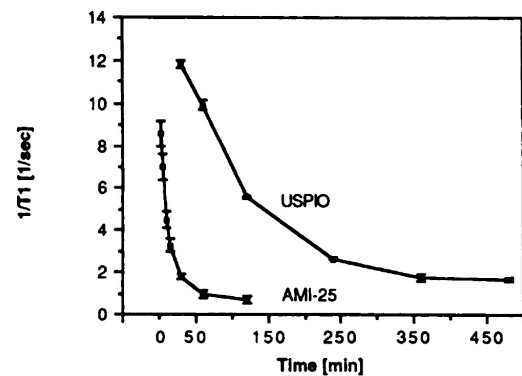
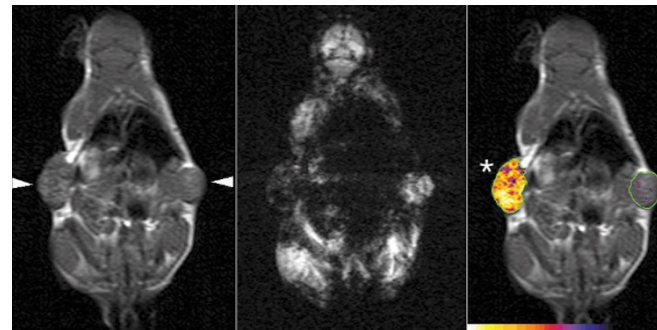
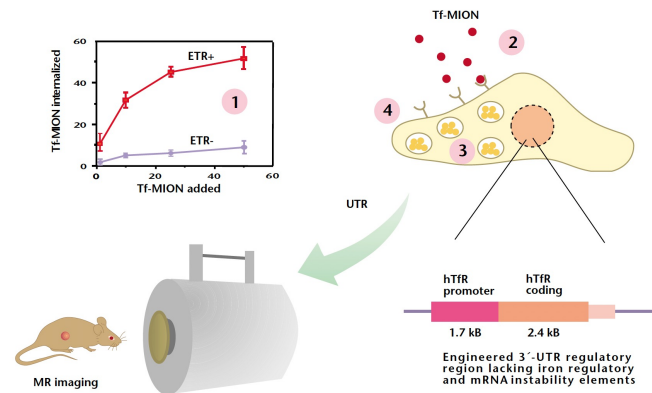


Figure 1. Blood clearance of USPIO and AMI-25. Means and SEMs of data from six animals are shown for each contrast medium. The calculated blood half-life of USPIO was 81 minutes, and that of AMI-25 was 6 minutes.



Weissleder et al. *Radiology* 1990
Weissleder et al *Nat Med* 2000



Memorial Sloan Kettering
Cancer Center

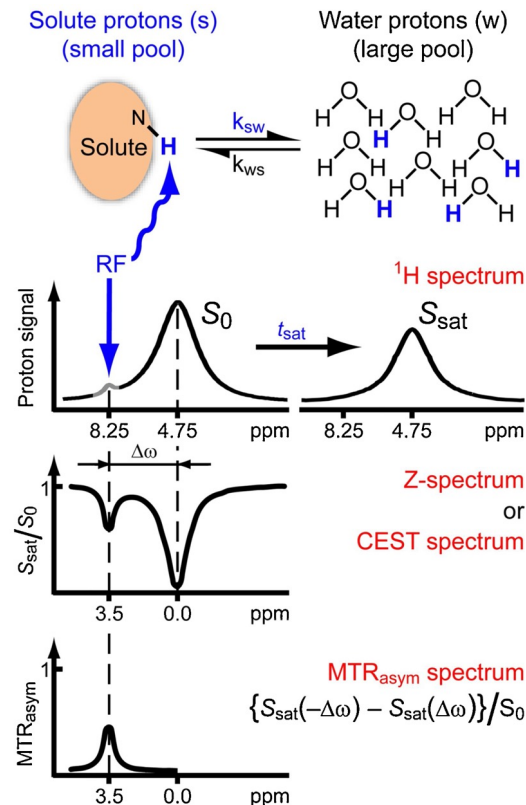
Contrast Mechanisms for MRI

- a. Relaxation based (small and large molecules)
- b. Chemical Exchange Saturation Transfer
- c. Magnetic Resonance Spectroscopy/Spectroscopic Imaging
- d. Multi-nuclear MRS/MRI
 - Isotope tracing
 - Hyperpolarization

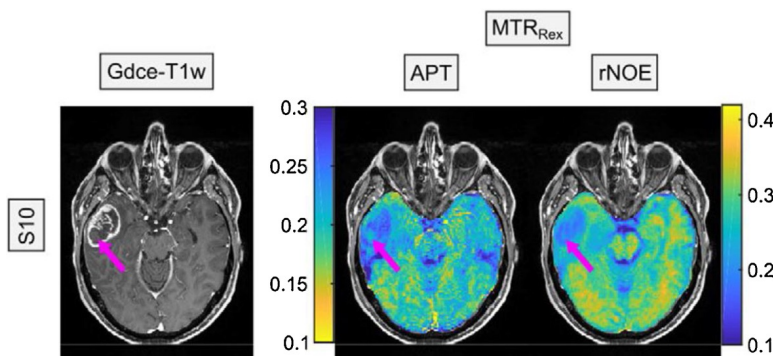


Memorial Sloan Kettering
Cancer Center

Chemical Exchange Saturation Transfer (CEST)

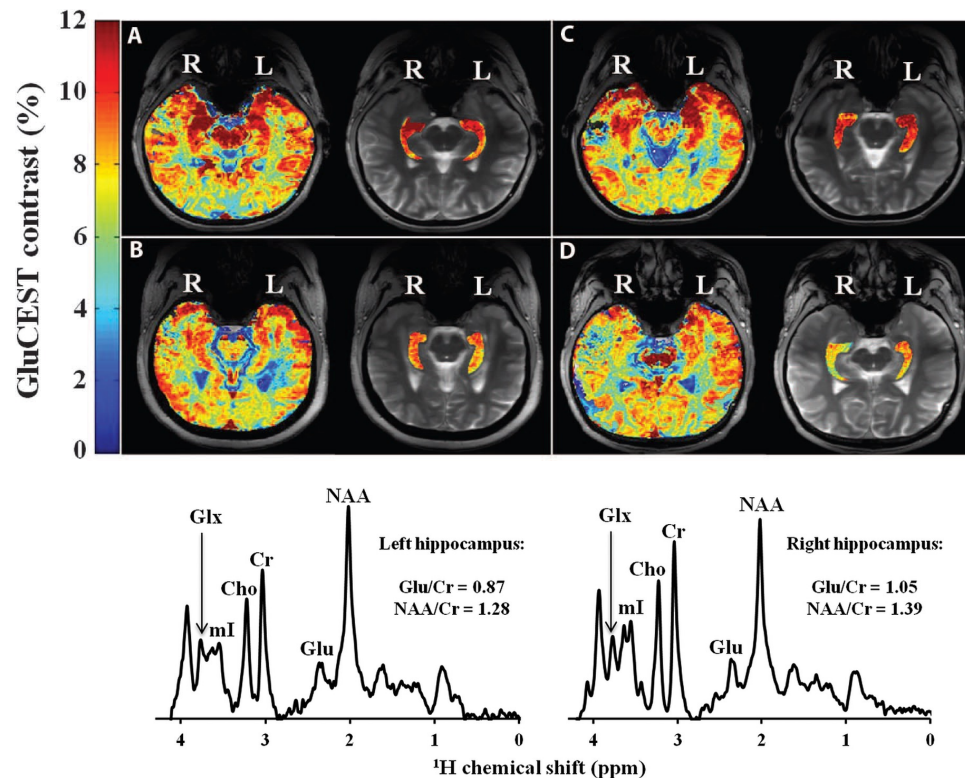


Technique	CEST agents	Chemical groups	Chemical Shift	Application
APT	Mobile proteins and peptides	Amide (N—H)	~3.5 ppm	Strokes (ischemic and hemorrhagic) Tumors Neurodegenerative diseases
GluCEST	Glutamate	Amine (N—H ₂)	~3 ppm	Neurodegenerative diseases, monitoring,
GlucoCEST	Glucose	—Hydroxyl (OH)	3 peaks [1.2 / 2.2/ 2.8 ppm]	Tumors
MICEST	Myo-inositol	Hydroxyl (O—H)	3 peaks [0.8 / 0.9 / 1.1 ppm]	Neurodegenerative diseases
CrCEST	Creatine	Amine (N—H ₂)	~1.8 ppm	Tumors, seizures



Mamoune et al. *J Chem Neuroanatomy* 2021
Goerke et al. *MRM* 2019

Endogenous Glutamate CEST



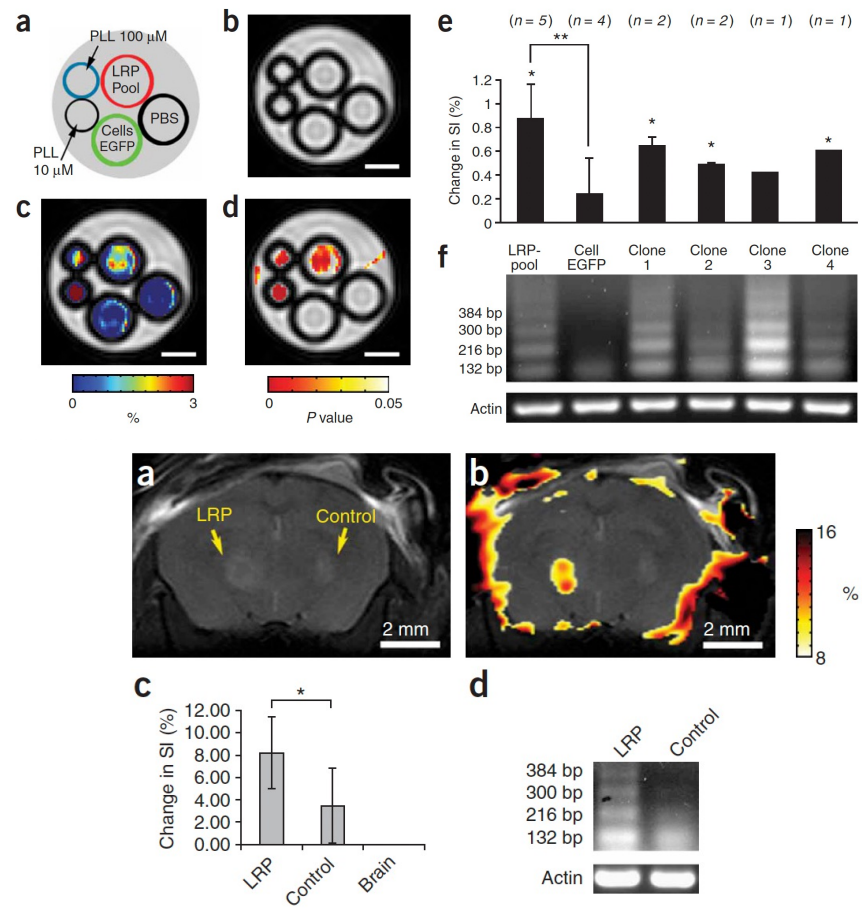
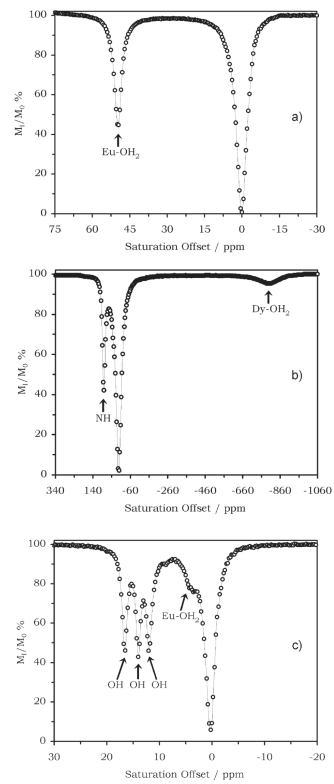
MRS confirmation for Right temporal lobe epilepsy (TLE)

Davis et al *Sci Transl Med* 2015



Memorial Sloan Kettering
Cancer Center

PARACEST



Woods et al *Chem Soc Rev* 2006
 Gilad et al. *Nat Biotech* 2007



Memorial Sloan Kettering
 Cancer Center

Contrast Mechanisms for MRI

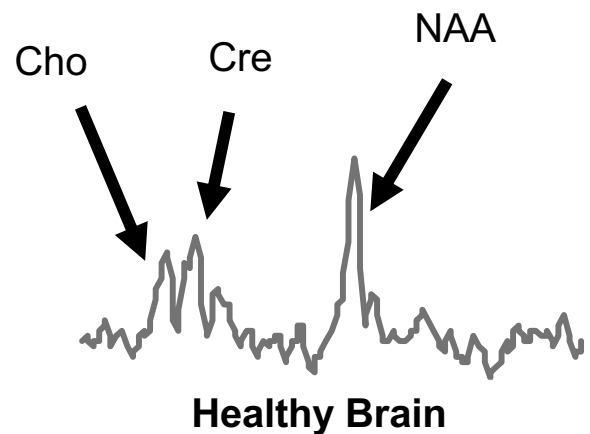
- a. Relaxation based (small and large molecules)
- b. Chemical Exchange Saturation Transfer
- c. Magnetic Resonance Spectroscopy/Spectroscopic Imaging
- d. Multi-nuclear MRS/MRI
 - Isotope tracing
 - Hyperpolarization



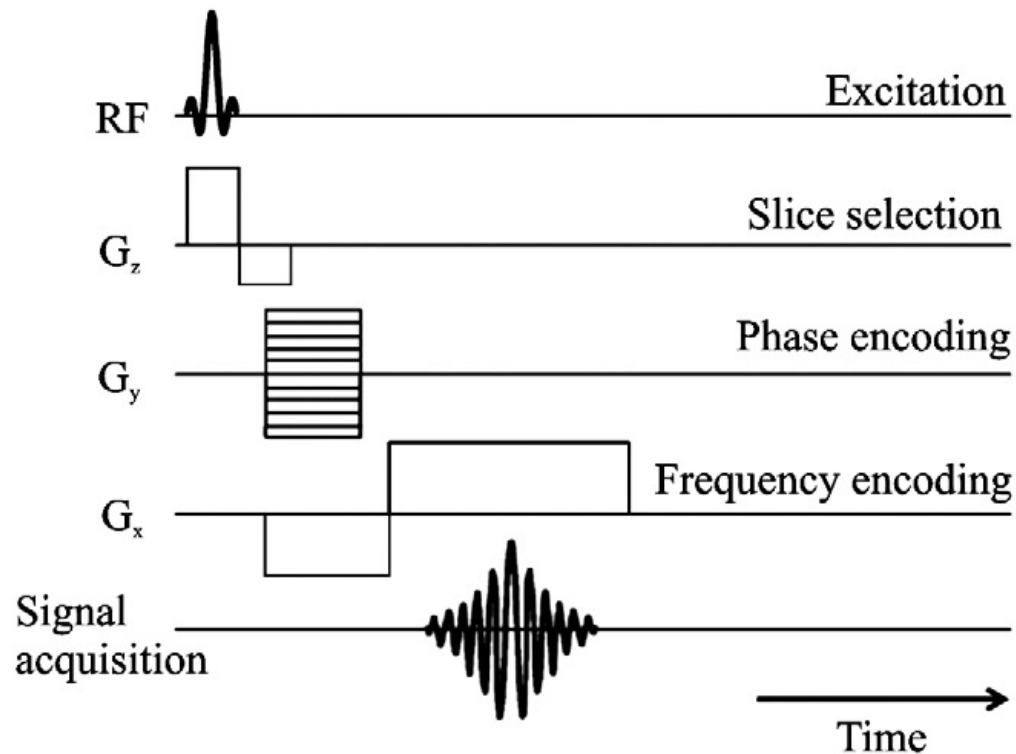
Memorial Sloan Kettering
Cancer Center

MR Spectroscopic Imaging (MRSI)

- What about detecting metabolites as opposed to structure?
 - MRI - mainly water 55 M, MRSI – metabolites ~5mM
→ Signal ~ 10,000x smaller!
 - End up w/ lower spatial resolution, longer scans but adds a new dimension

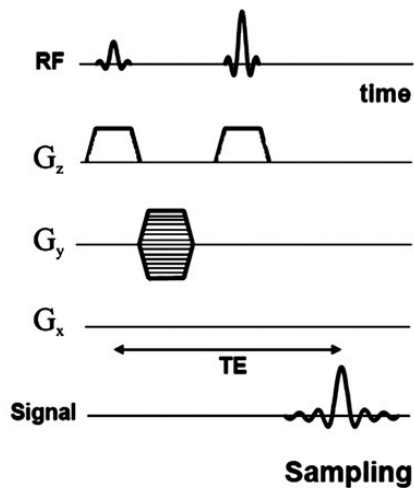


How do you localize MRS?

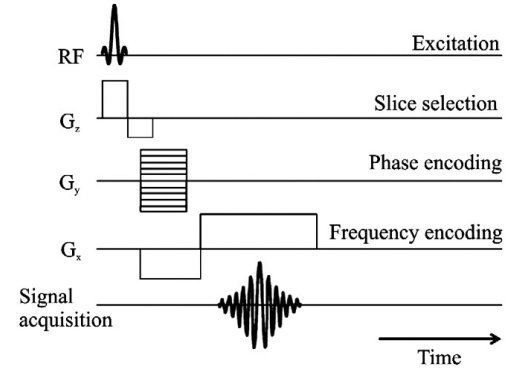
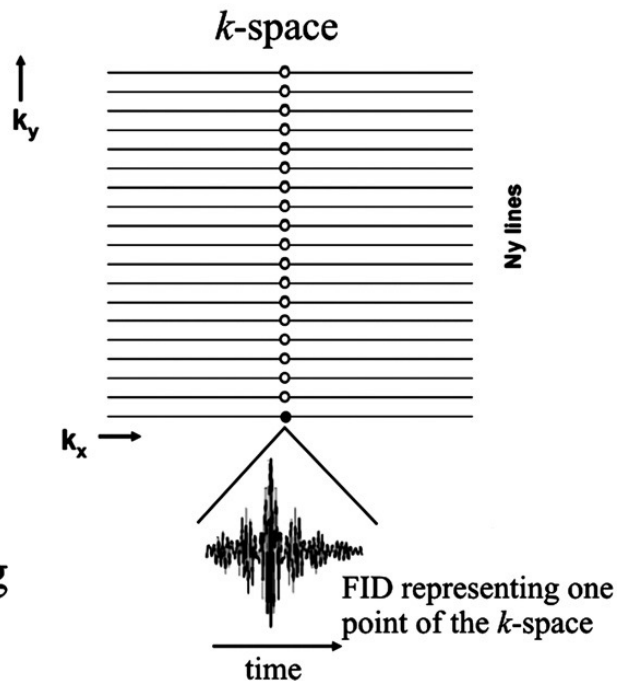


Memorial Sloan Kettering
Cancer Center

How do you localize MRS?



1D Spectroscopic imaging

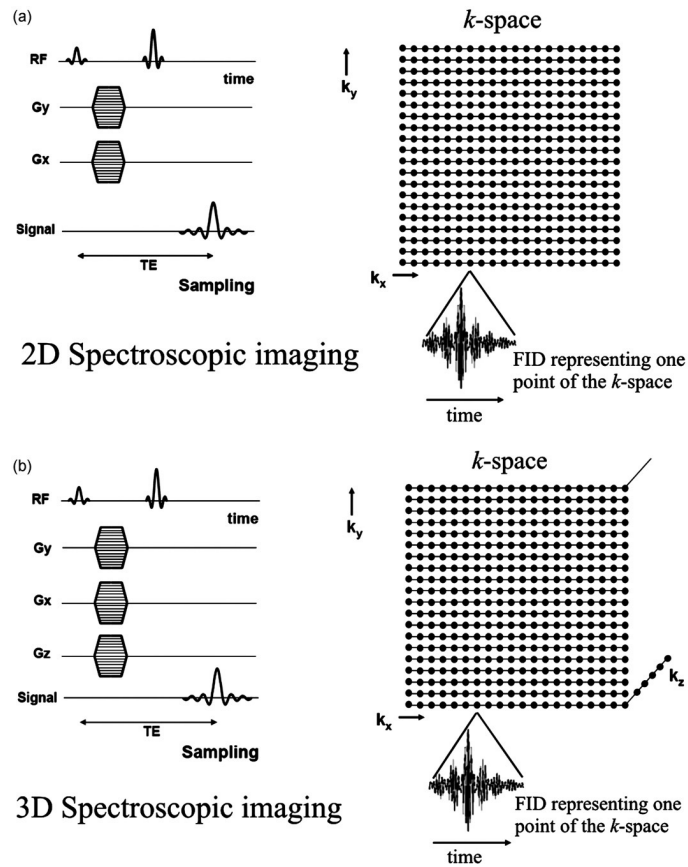


Skoch et al. *Euro J of Rad* 2008



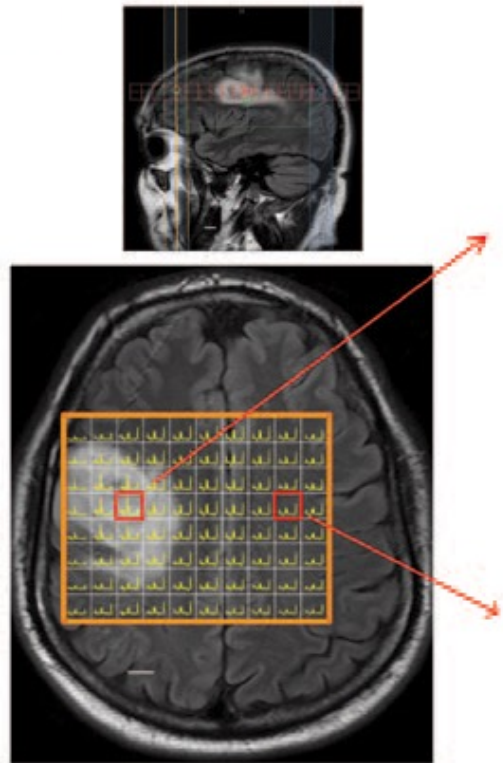
Memorial Sloan Kettering
Cancer Center

How do you localize MRS?



Memorial Sloan Kettering
Cancer Center

Steady state pool sizes ^1H MRSI

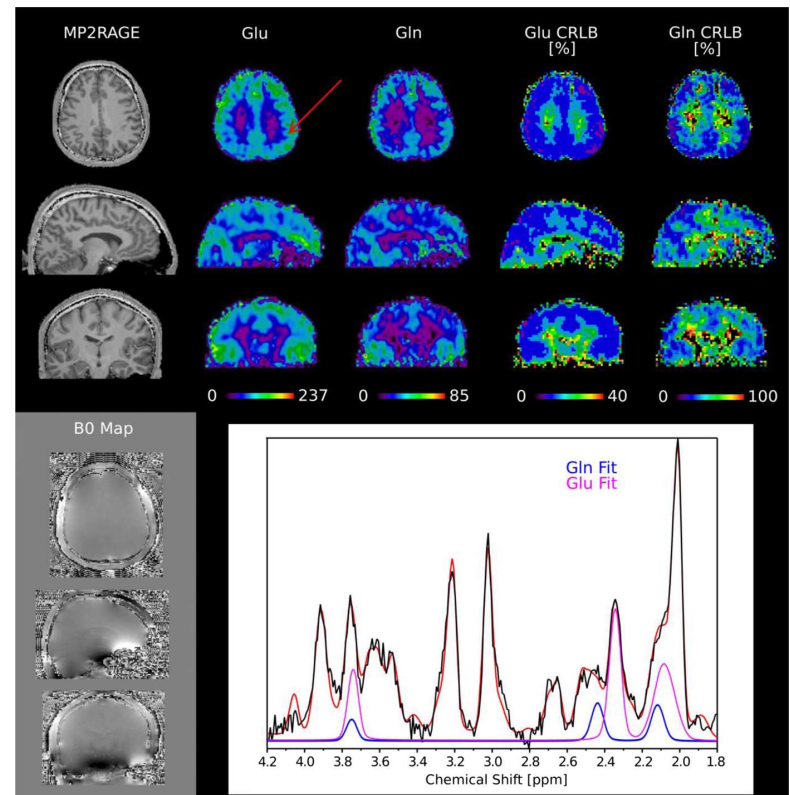
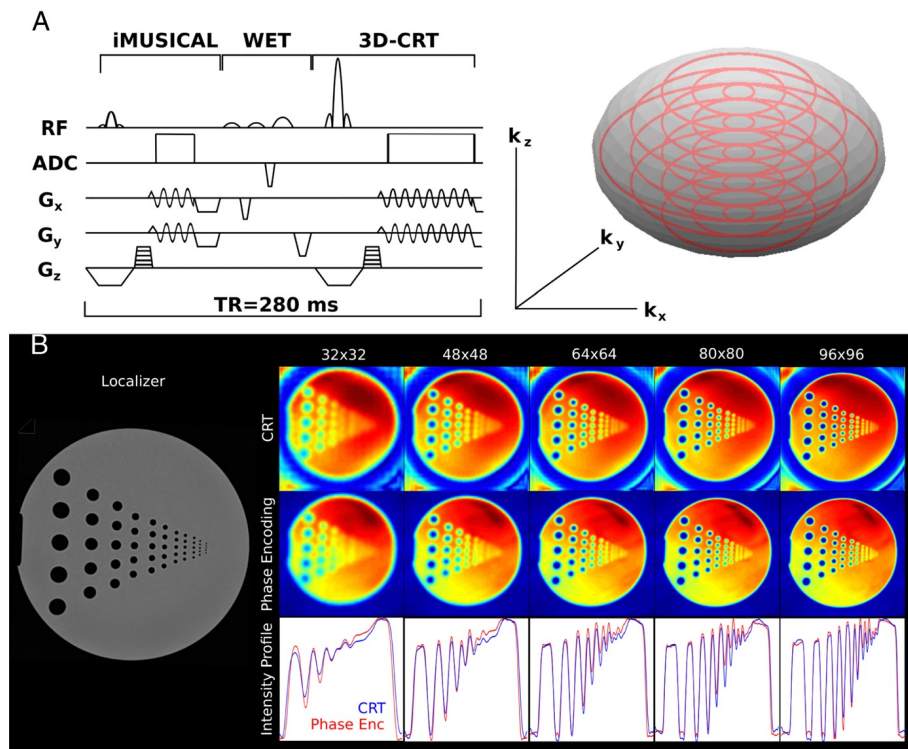


Choi et al *Nature Med* 2012



Memorial Sloan Kettering
Cancer Center

High-res 3D MRSI

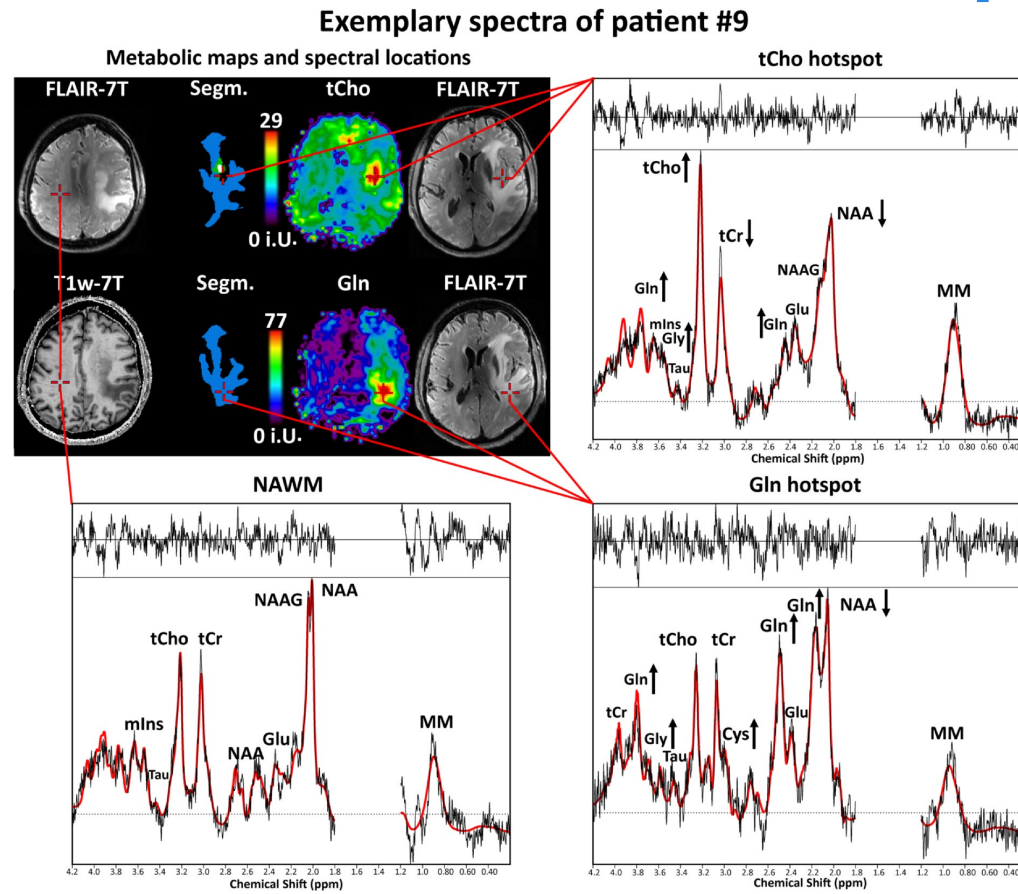


Hingerl et al *Invest Rad* 2020



Memorial Sloan Kettering
Cancer Center

High-res 3D MRSI – brain tumor patient



Hangel et al *NeuroImage* 2020



Memorial Sloan Kettering
Cancer Center

Contrast Mechanisms for MRI

- a. Relaxation based (small and large molecules)
- b. Chemical Exchange Saturation Transfer
- c. Magnetic Resonance Spectroscopy/Spectroscopic Imaging
- d. Multi-nuclear MRS/MRI
 - Isotope tracing
 - Hyperpolarization

NMR/MRI active nuclei

Nuclei	<i>m</i> (spin)	Natural abundance (%)	γ (rel to ^1H)	$\Delta\delta$ (ppm)	T_1 range	Example biomedical application
^1H	1/2	99.98	1	13	0.1–2 s	Total body MRI and MRSI
^2H	1	0.02	0.1535	13	<1 s	Metabolic tracer injection using MRSI
^{13}C	1/2	1.11	0.2515	200	0.1–100 s	Metabolic tracer injection using MRSI
^{15}N	1/2	0.37	0.1013	900	0.1–400 s	Metabolic tracer injection using MRSI
^{17}O	5/2	0.04	0.1355	1160	5–50 ms	Oxidative metabolism using MRSI
^{19}F	1/2	100.00	0.9409	700	0.1–1 s	Tracer injection of therapies using MRSI
^{23}Na	3/2	100.00	0.2645	72	10–50 ms	Neurodegeneration and cardiac using MRI
^{31}P	1/2	100.00	0.4048	430	0.05–2 s	Bioenergetics and pH using MRSI

MRI – magnetic resonance imaging, MRSI – magnetic resonance spectroscopic imaging, *m* – quantum spin number, γ – gyromagnetic ratio, $\Delta\delta$ – chemical shift.



Memorial Sloan Kettering
Cancer Center

pH – ^{31}P Spectroscopy

Intracellular pH (Moon and Richards 1973) and extracellular pH (Myer et al 1985) using chemical shift

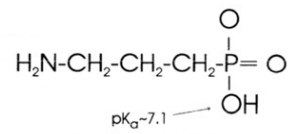
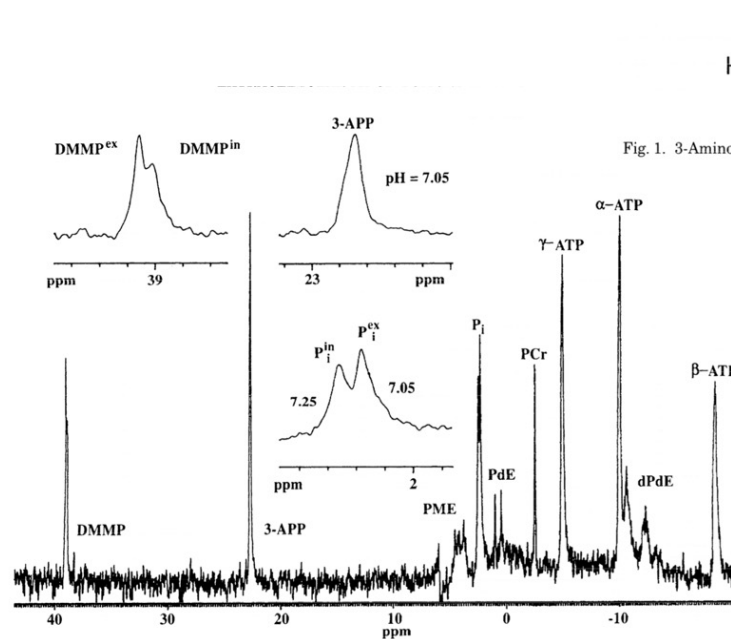
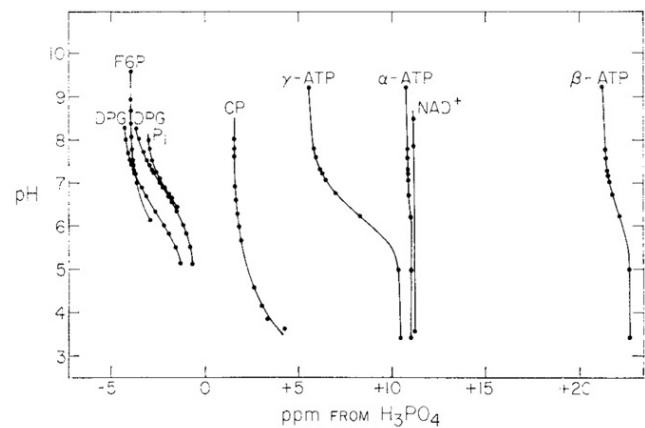
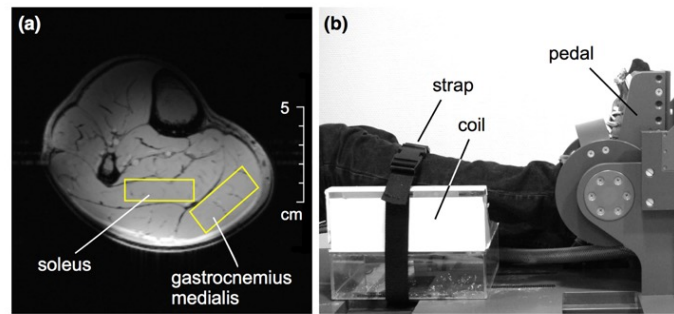


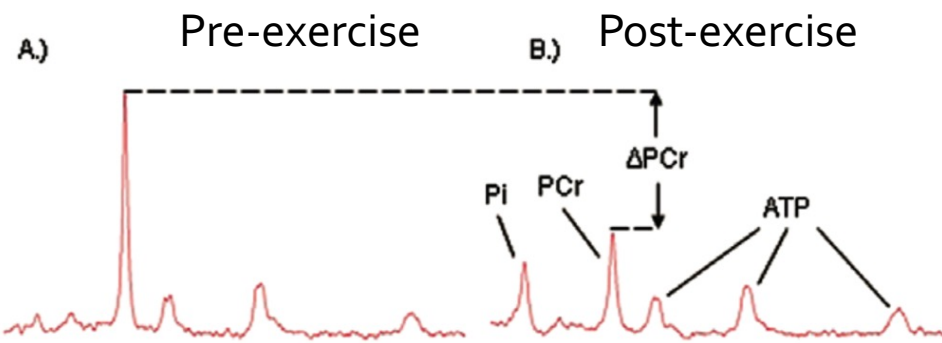
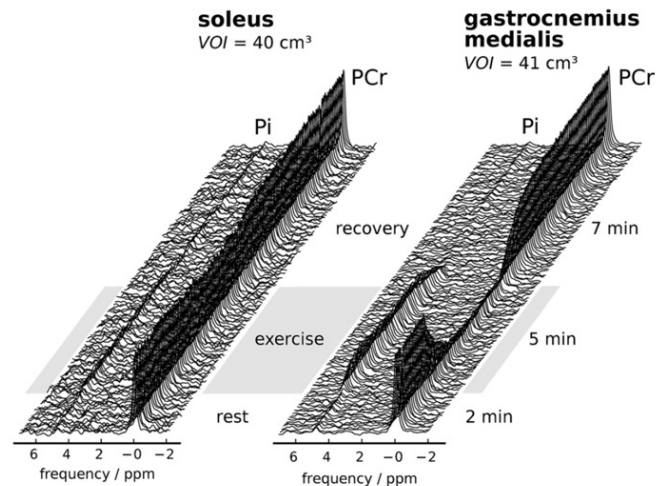
Fig. 1. 3-Aminopropylphosphonate (3-APP).



Bioenergetics – ^{31}P MR Spectroscopy



Localized ^{31}P MR spectra (single acquisitions)



Fiedler et al 2015



Memorial Sloan Kettering
Cancer Center

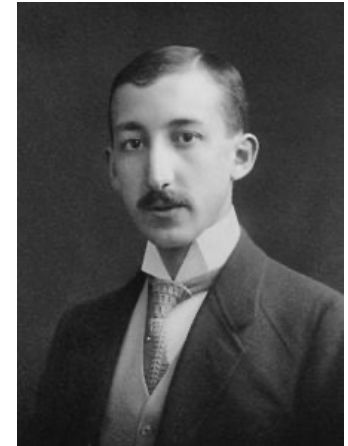
Isotope Tracing?



Memorial Sloan Kettering
Cancer Center

First isotope tracing studies

- Radioactive isotopes were first used in biological systems in the 1920s by George de Hevesy, who won the Nobel Prize in Chemistry in 1943 - Traced using ^{212}Pb into *Vicia faba* (horse-bean)¹
- Later the first stable isotopes were used for tracing, including ^2H tracing by Schoenheimer²
- This lead to isolated organs, particularly the heart, and to translate isotopic labeling data into relative or absolute metabolic fluxes³
- Used in humans since 1934, when Hevesy and Hofer used deuterium oxide to estimate the size of the whole-body water pool and rate of water elimination⁴



¹Hevesy Biochem J 1923

²Schoenheimer et al. *Science* 1935, *J Biochem* 1936

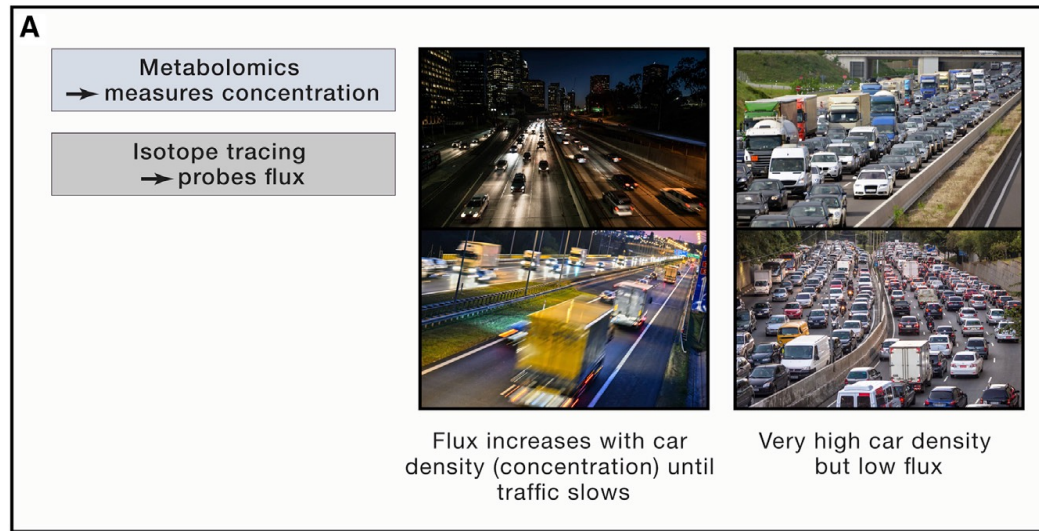
³Chance et al. 1983, Malloy et al. 1987, Russel et al 1997

⁴Hevesy and Hofer *Nature* 1934



Memorial Sloan Kettering
Cancer Center

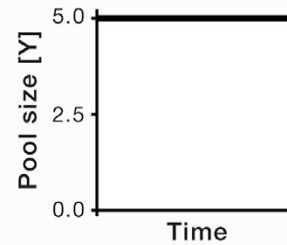
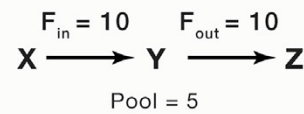
Pool size versus Flux



A Metabolic steady state

- Pool size does not change
- Flux is balanced

$$F_{in} = F_{out}$$



Early MRS leveraged isotope tracing and NMR

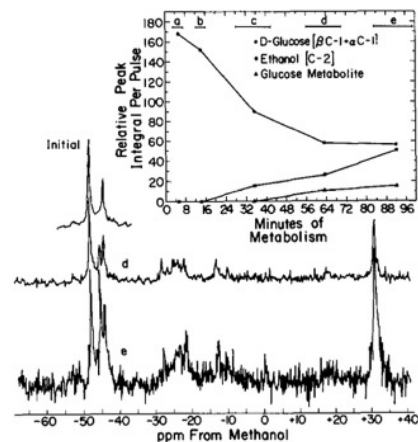


Fig. 3. Metabolism of $[1-^{13}\text{C}]$ glucose. a) 500 pulses, 3–7 m after initiation of metabolism; b) 500 pulses, 12–16 min; c) 1500 pulses, 28–42 min; d) 1500 pulses, 56–70 min; e) 151 pulses, 83–99 min. The spectra obtained during the initial time periods show only the signals corresponding to the substrate, $[1-^{13}\text{C}]$ glucose. The C-1 region is illustrated. Spectra generated during the time periods (d) and (e) are illustrated for the region between 40 ppm and -65 ppm. Signals in the region between -12 ppm and -28 ppm are generated from the natural abundance ^{13}C in glucose carbon atoms other than C-1.

Eakin et al. *FEBS Letters* 1972

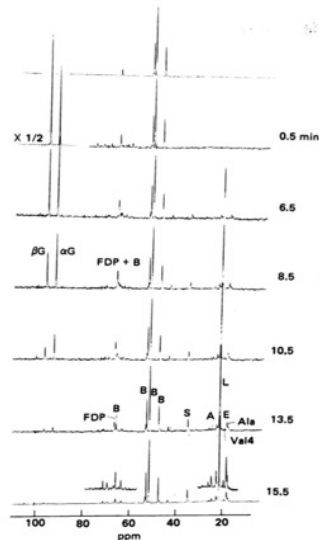


Fig. 1. The 90.52-MHz ^{13}C NMR spectra of anaerobic *E. coli* cells at 20°C as a function of time from ^{13}C -1 glucose addition. The cells were suspended in 10 mM Na_2HPO_4 , 10 mM KH_2PO_4 , 200 mM 1,4-piperazine diethanesulfonic acid (Pipes)/50 mM 2-(N-morpholino)ethanesulfonic acid (Mes), pH 7.0, 10% v/v with 10% NaOH at a density of $\sim 6 \times 10^{11}$ cells/ml. $[1-^{13}\text{C}]$ Glucose was added to a final concentration of 50 mM in the NMR sample, at time 0. The first spectrum (1600 scans) shows the natural-abundance ^{13}C peaks (assigned to the Pipes and Mes buffers) detectable in the suspension prior to glucose addition. All subsequent spectra, except the last one, represent 200 free induction decays accumulated in 1 min. The last spectrum consists of 1600 scans. The time given for each spectrum indicates the middle of the accumulation period, referred to glucose addition. FDP, Fru-1,6-P₂; see text for other abbreviations.

Ugurbil et al. *PNAS* 1978

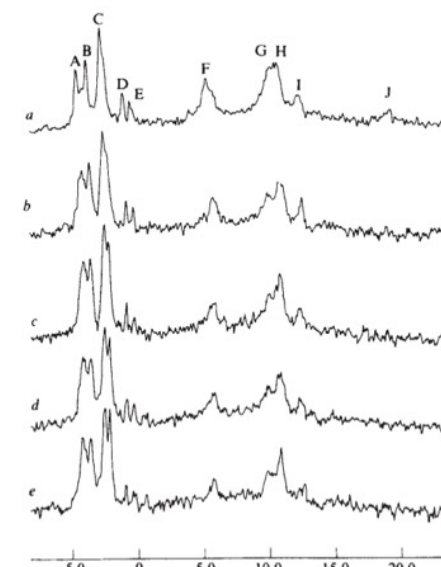


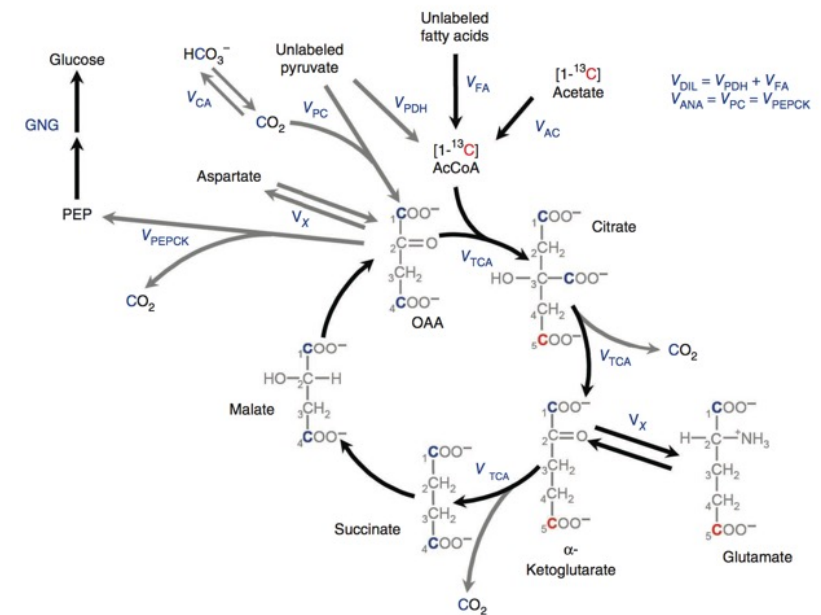
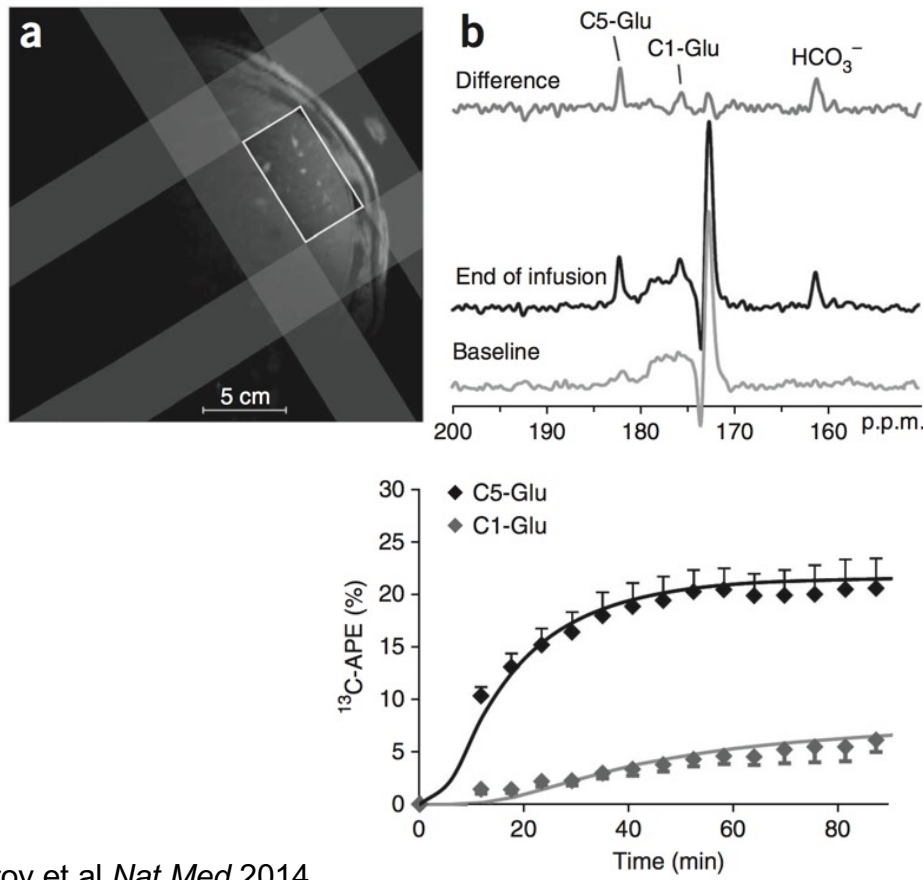
Fig. 1 NMR spectra at 145.7 MHz of ^{31}P nuclei in isolated rat liver cells. of 1,000 pulses of 60° free induction decays of 0.34s duration obtained with fasted for 24 h were used for the isolation of the liver cells. The cells were prep

Cohen et al. *Nature* 1978



Memorial Sloan Kettering
Cancer Center

¹³C-acetate MR Spectroscopy



Befroy et al *Nat Med* 2014



Memorial Sloan Kettering
Cancer Center

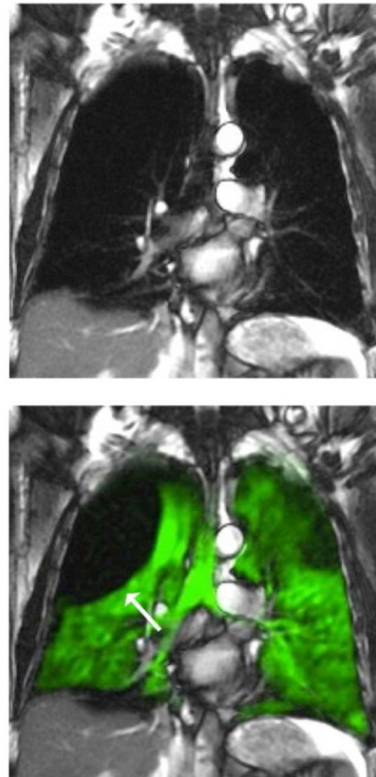
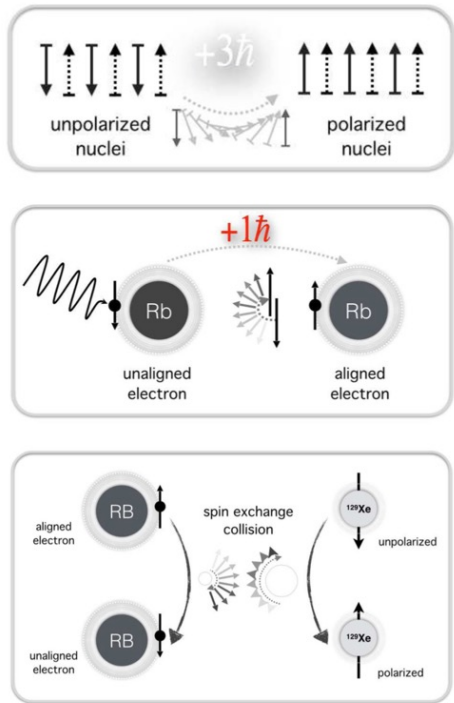
Hyperpolarized MRI

- What's wrong with MRI? – Signal is weak!
- Multiple Methods to increase it for high SNR MRI:
 - **Optical pumping** (^3He , ^{129}Xe)
 - **Chemical reduction using Parahydrogen** (PHIP, SABRE)
 - **Dynamic nuclear polarization** (dissolution DNP, solid state DNP)



Memorial Sloan Kettering
Cancer Center

HP MRI of gases



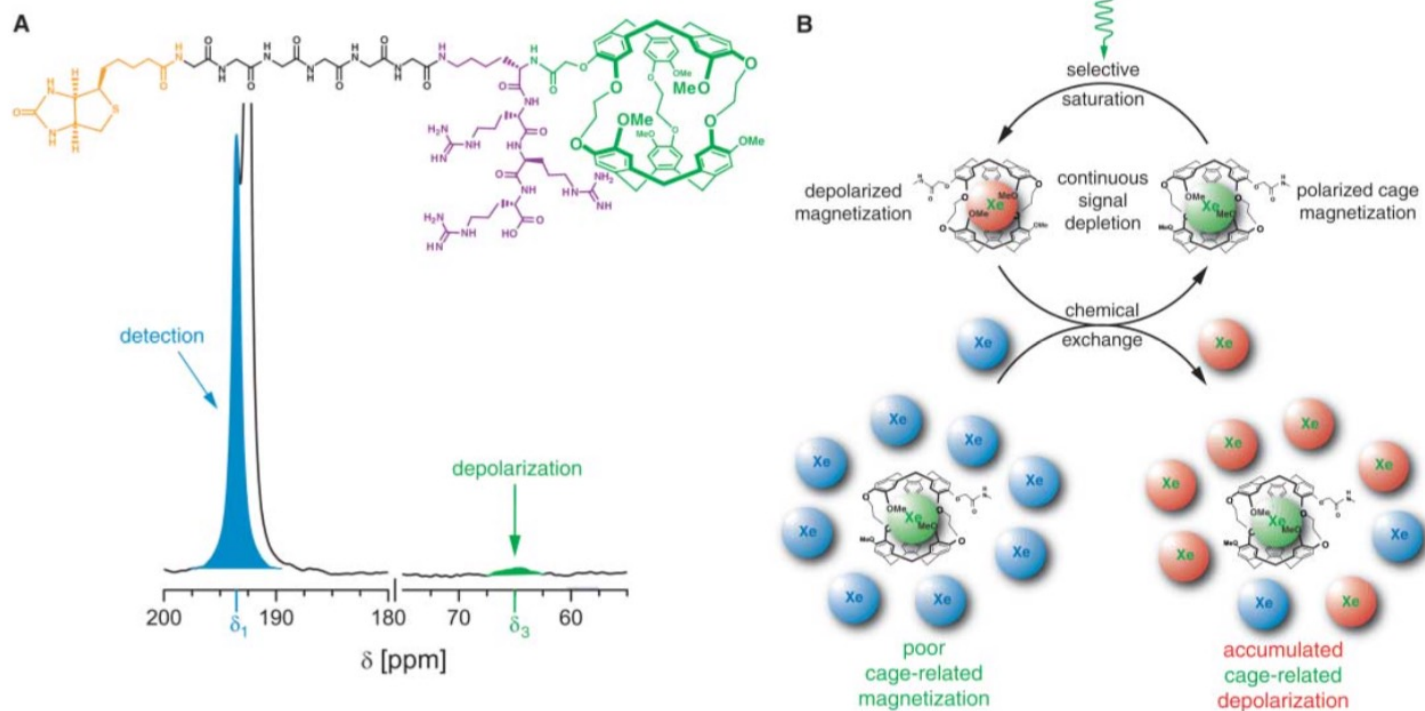
Roos et al. *Magn Reson Imaging Clin N Am* 2015



Memorial Sloan Kettering
Cancer Center

HP MRI of gases (HyperCEST)

REFURGI

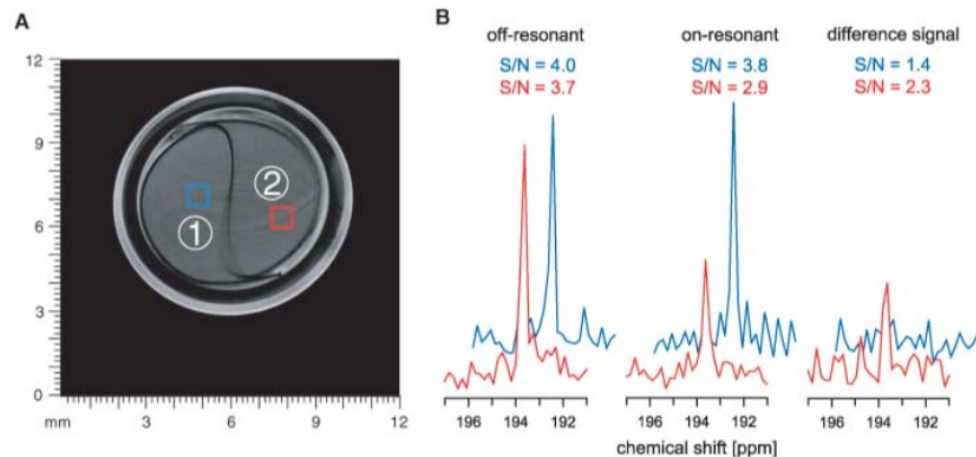


Schroeder et al. *Science* 2006

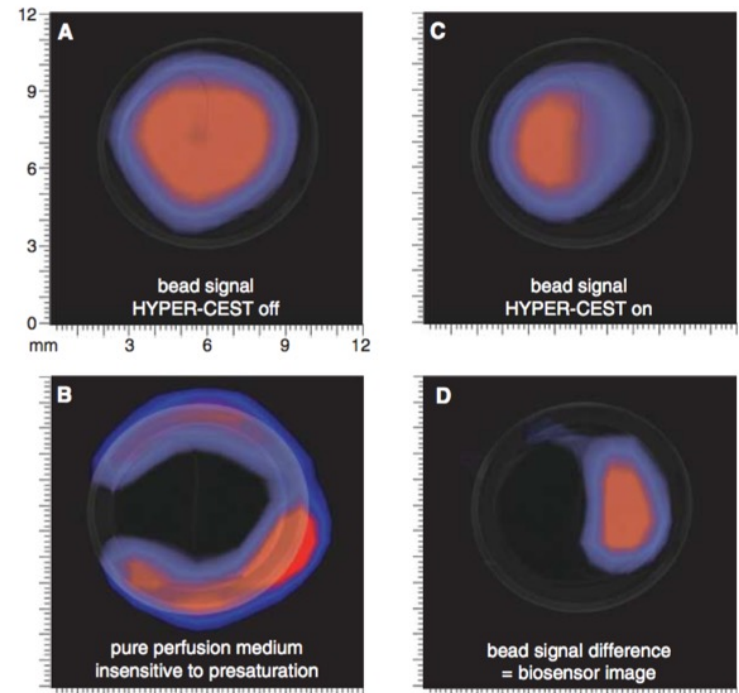


Memorial Sloan Kettering
Cancer Center

HP MRI of gases (HyperCEST)



Biosensor is only in volume 2



Schroeder et al. *Science* 2006

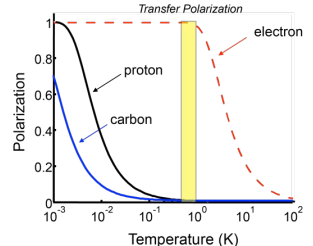


Memorial Sloan Kettering
Cancer Center

How do we overcome the limited sensitivity of magnetic resonance for isotope tracing in liquids?

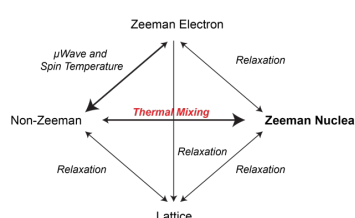
Dynamic Nuclear Polarization

Transfer polarization to nucleus of interest



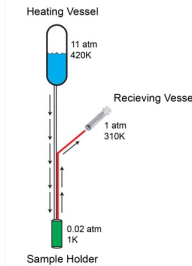
Overhauser 1952

Mechanism for polarization propagation



Abragam and Goldman 1955
Borghini 1968

Dissolution Process



Ardenkjaer-Larsen, Golman et al. 2003

Parahydrogen Induced Polarization

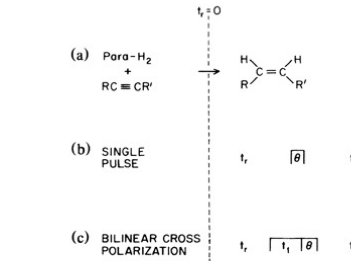
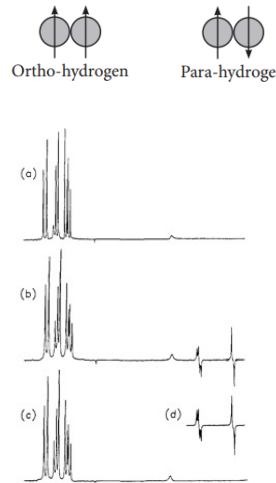
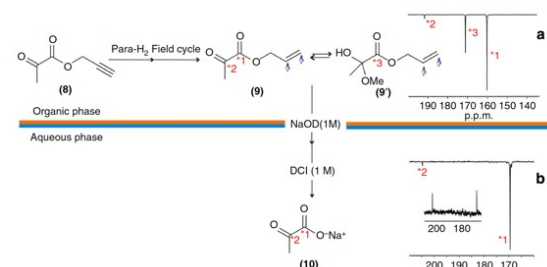


FIG. 1. Sequence of events for conversion of the spin order of parahydrogen to magnetization. The origin of time is the addition of molecular hydrogen to a suitable acceptor, as shown, for example, in (a). In (b) a brief mixing pulse of nutation angle θ at the proton Larmor frequency is delivered at a time t_r after the reaction to elicit development of transverse magnetization during t_2 . In (c) the mixing pulse is preceded by a cross-polarization sequence of length t_1 to share the spin order with weakly coupled resonances.

Figure 1. Demonstration that parahydrogen is a synthon for dramatically enhanced nuclear alignment. Part (a) shows the proton NMR spectrum prior to the reaction. The intense lines are due to the acrylonitrile substrate. Part (b) was obtained subsequent to the hydrogenation to propiophenone but prior to spin-lattice equilibration. The large antiphase propiophenone signal in response to a $\pi/4$ pulse are observed only with parahydrogen and H₂ as reagent. Part (c) shows the spectrum of the equilibrated sample and shows that the signal of (b) was a large transient enhancement. Part (d) is a line shape simulation demonstrating the agreement of the theory of ref 1 with the experiment of part (b). The line width is 3.5 Hz due to inhomogeneity of the field, which is degraded by the H₂ capillary.

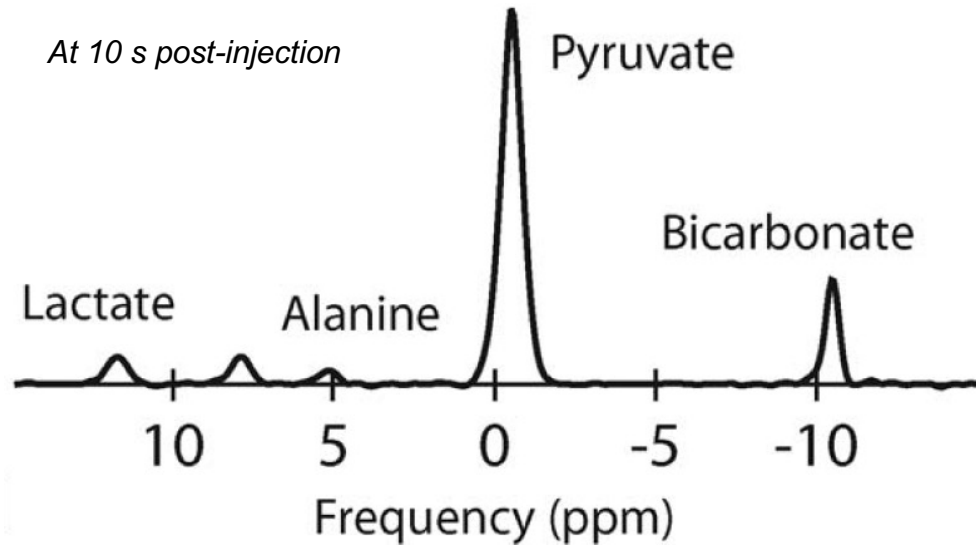
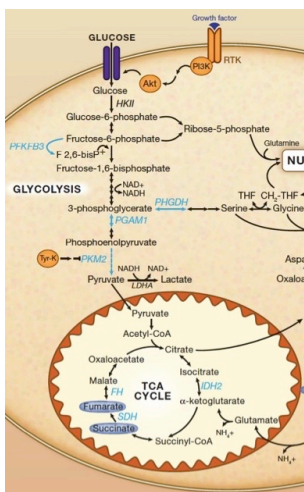
Bowers and Weitekamp 1986,1987



Reineri, Aime et al. 2015

Hyperpolarized ^{13}C Magnetic Resonance

- HP MRI provides a mechanism to overcome the sensitivity problem of MR by aligning spins outside of the magnet
- Follow the conversion of **HP pyruvate** through many pathways in seconds!
 - Reduction to **HP Lactate**
 - Transamination to **HP Alanine**
 - Decarboxylation to **HP carbon dioxide** and later **bicarbonate (pH)**



Keshari and Wilson *Chem Soc Rev* 2014

Memorial Sloan Kettering
Cancer Center

Many probes and methods can be developed to interrogate metabolism

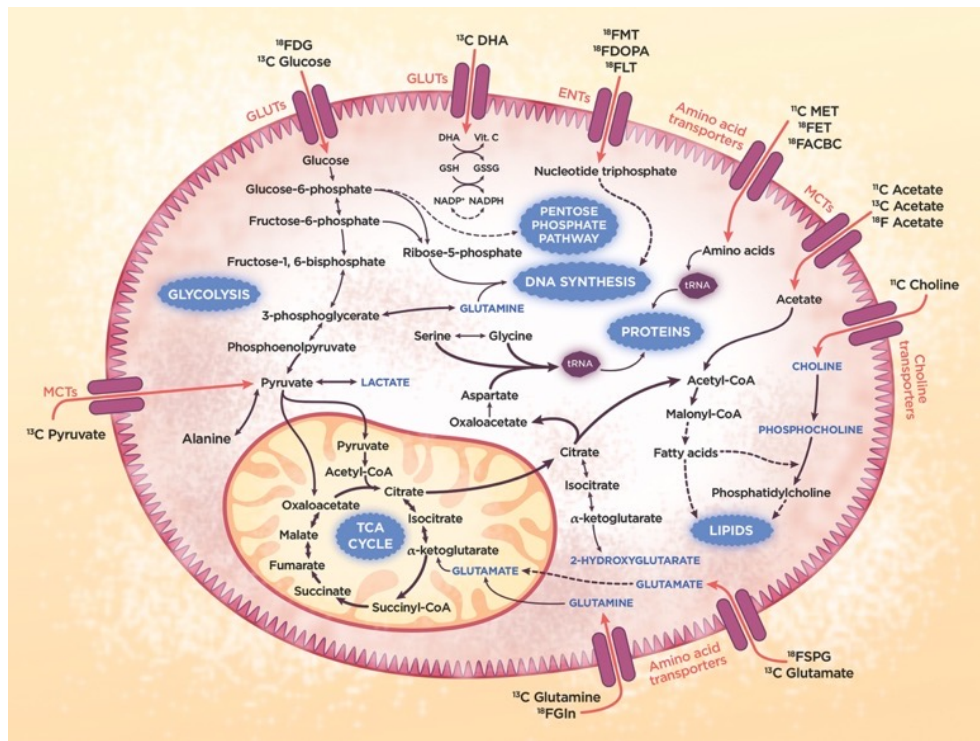


Table 3 Chemical structures of HP probes

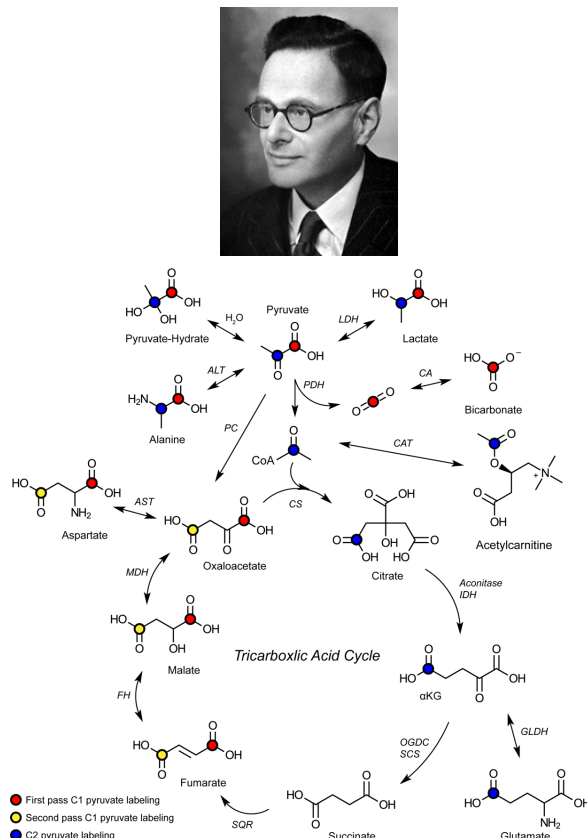
Chemical structure	Index	HP agent	MW (Da)	Apparent T_1 (s)	Application	Ref.
	1	^{14}C sodium formate	69	20 (9.4 T)	C	222
	2	$[1,1^{14}\text{C}]$ glycine	76	50 (9.4 T)	C	78
	3	$[1,1^{14}\text{C}]$ sodium acetate	83	40 (3 T); 46 (14.1 T)	A, C	121, 223 and 224
	4	$[1,1^{14}\text{C}]$ sodium bicarbonate	85	49 (11.7 T); 50 (3 T); 34 (3 T)	A, C	83 and 177
	5	$[1,1^{14}\text{C}, \text{H}_2]$ sodium acetate	86	50 (14.1 T)	C	121
	6	$[1,1^{14}\text{C}]$ pyruvic acid	89	67 (3 T); 48 (11.7 T); 44 (14.1 T)	A, B, C	83 and 121
	6	C ₆ of $[1,2^{14}\text{C}]$ pyruvic acid	90	56 (3 T)	A, C	177
	7	$[1,1^{14}\text{C}]$ alanine	90	42 (3 T); 29 (9.4 T)	A, C	78 and 225
	8	$[1,1^{14}\text{C}]$ sodium propionate	97	NR	A, C	224
	9	$[1,1^{14}\text{C}]$ sodium pyruvate	106	23 (9.4 T)	C	78
	10	$[1,1^{14}\text{C}]$ sodium butyrate	111	43 (14.1 T)	C	226
	11	$[1,1^{14}\text{C}]$ sodium lactate	113	45, 50.6 (3 T); 32, 33.4 (14.1 T)	A, C	52 and 227
	12	$[1,4^{14}\text{C}]$ fumaric acid	118	24 (9.4 T); 29 (11.7 T)	A, B, C	83 and 196
	13	C ₆ of benzoic acid	122	35 (11.7 T)	C	54
	14	$[1,1^{14}\text{C}]$ glycine	122	30 (3 T)	C	78
	13	$[1,1^{14}\text{C}]$ benzoic acid	123	35 (11.7 T)	C	54
	15	$[1,1^{14}\text{C}]$ ketosuccinic acid	131	55 (9.4 T)	A, C	169
	16	$[1,1^{14}\text{C}]$ leucine	132	24 (9.4 T)	C	78
	17	$[1,1^{14}\text{C}]$ aspartic acid	134	29 (9.4 T)	C	78
	18	C ₆ of $[1,2^{14}\text{C}]$ salicylic acid	138	NR	C	38
	19	$[1,1^{14}\text{C}]$ ornithine	147	25 (9.4 T)	C	78
	20	$[1,1^{14}\text{C}]$ tyrosine	147	26 (9.4 T)	C	78
	21	$[1,1^{14}\text{C}]$ glutamate	148	26 (9.4 T); 34 (9.4 T) FG	A, C	78
	22	$[1,1^{14}\text{C}]$ methionine	150	17 (9.4 T)	C	78
	23	$[1,1^{14}\text{C}]$ N-acetyl-methionine	192	28 (3 T)	A, B, C	188
	4	$[1,1^{14}\text{C}]$ sodium bicarbonate	195	NR	A, C	37
	24	2-Naphthaleneacetic acid-6-methoxy-2-methyl (NA)	230	15 (11.7 T)	C	54
	25	$[2,2^{14}\text{C}]$ diacetyl	88	30 (7 T)	C	39
	6	$[2,1^{14}\text{C}]$ pyruvic acid	89	NR	B, C	84
	6	C ₂ of $[1,2^{14}\text{C}]$ pyruvic acid	90	44 (3 T)	A, C	177
	26	$[2,1^{14}\text{C}]$ benzoylformic acid	151	24 (11.7 T); 19 (14.1 T)	C	35
	27	$[1,1^{14}\text{C}]$ ethyl pyruvate	117	45 (3 T)	A, C	87
	28	Ethyl-2-oxopyruvate (NA)	125	NR	C	132
	28	$[1,1^{14}\text{C}]$ diethyl oxalate	148	22 (8.4 T)	C	126
	29	$[1,1^{14}\text{C}]$ dehydrofructose acid	175	56 (3 T); 21 (9.4 T); 21 (11.7 T)	A, B, C	85 and 86
	31	C ₆ of ascorbic acid (NA)	176	NR	C	38
	31	$[1,1^{14}\text{C}]$ ascorbic acid	177	29 (3 T); 16 (9.4 T); 16 (11.7 T)	A, B, C	85 and 86
	32	Methyl fumarate (NA)	193	NR	C	132
	33	C ₆ -methyl-isopropyl-1,2, ¹⁴ C-oxalate- ² H ₁₈	234	34 (4.7 T)	C	128
	34	Ns-benzyloxymethyl-2-methyl ester	196	NR	C	228
	35	$[1,1^{14}\text{C}]$ acetic anhydride	104	34 (11.7 T); 45, 50 (14.1 T)	C	40
	36	$[1,1^{14}\text{C}, \text{H}_2]$ acetic anhydride	110	NR	C	121
	37	$[1,1^{14}\text{C}]$ butyric anhydride	160	39, 40 (14.1 T)	C	226
	38	¹⁴ Curea	61	44 (11.7 T); 35 (14.1 T)	A, C	83
	39	D(^{14}C)- ^{14}C glutamate	87	NR	C	85
	40	N(^{14}C)- ^{14}C glycine	118	15 (11.7 T); 17 (14.1 T)	C	40
	41	N(^{14}C)- ^{14}C alanine	132	15 (11.7 T)	C	40
	19	$[5,1^{14}\text{C}]$ glutamine	145	16 (9.4 T)	B, C	118
	42	N(^{14}C)- ^{14}C serine	148	11 (11.7 T)	C	40
	43	$[5,1^{14}\text{C}, \text{H}_2]$ glutamine	149	33 (9.4 T)	B, C	40

Tee and Keshari *Cancer J* 2015
 Keshari and Wilson *Chem Soc Rev* 2014

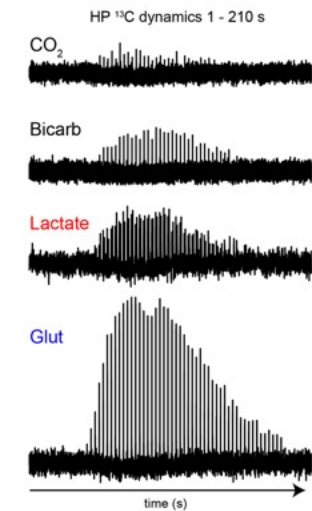
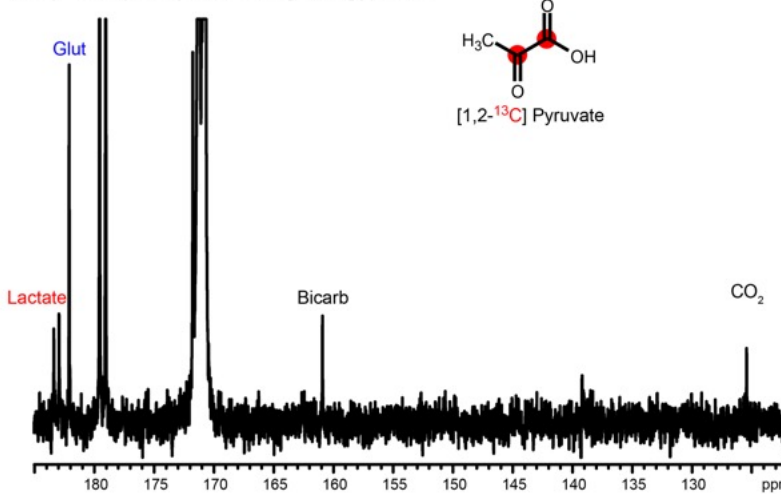


Memorial Sloan Kettering
 Cancer Center

Hyperpolarized ^{13}C NMR/MRI

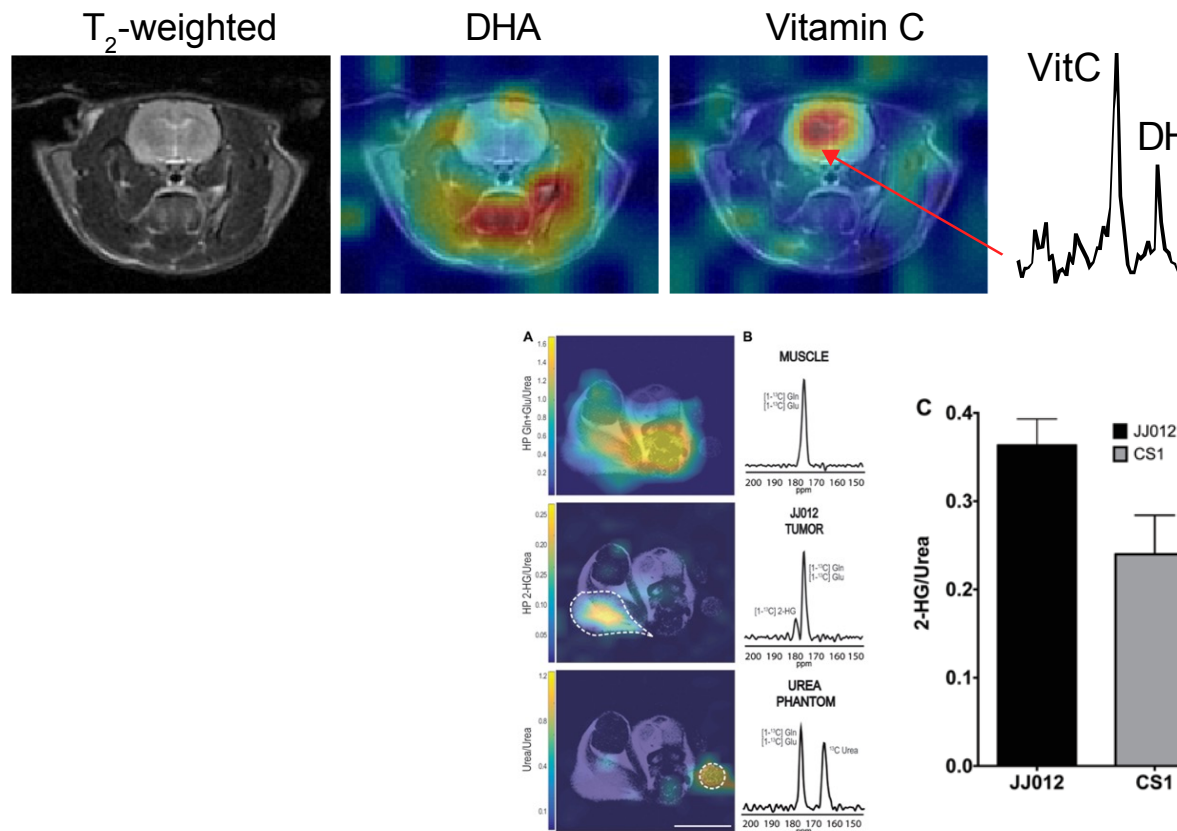


C. Dynamics post-injection of HP [1,2- ^{13}C] pyruvate



Memorial Sloan Kettering
Cancer Center

Hyperpolarized ^{13}C MRI



Keshari et al *PNAS* 2011

Salamanaca-Cardona et al. *Cell Metabolism* 2017

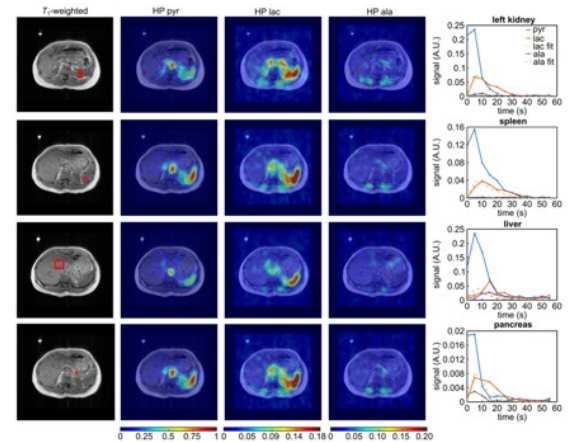
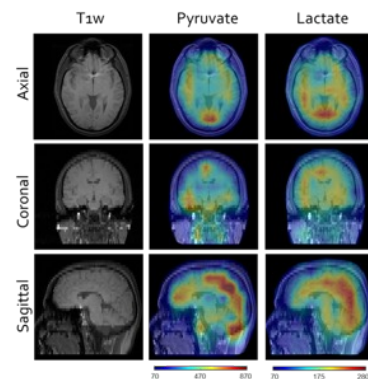
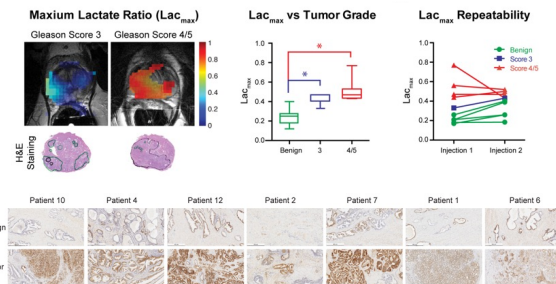


Memorial Sloan Kettering
Cancer Center

HP MRI in humans facilitates imaging isotope tracing

It turns out tumors make lactate...
and it might be rate limited by transport...

so do many organs (heart, brain etc)...



Miloushev et al. *Cancer Res* 2018
Granlund et al. *Cell Metabolism* 2020
Deh et al. *MRM* 2024
Zhang et al. *JMRI* 2024



Memorial Sloan Kettering
Cancer Center

Lets take a break



Paper discussion

2 Discussion Papers:

- Day, S. E. *et al.* Detecting tumor response to treatment using hyperpolarized ¹³C magnetic resonance imaging and spectroscopy. *Nat Med* **13**, 1382–1387 (2007).
- Choi, C. *et al.* 2-hydroxyglutarate detection by magnetic resonance spectroscopy in IDH-mutated patients with gliomas. *Nat Med* **18**, 624–629 (2012).



Memorial Sloan Kettering
Cancer Center